MB31

BOLOGNA SECTION

Paolo Finelli

University of Bologna

paolo.finelli@unibo.it

INFN-MB31 Collaboration Meeting in Trento - December 16/17, 2011

LATEST COMMENT OF THE MB31 REFEREES

…A lot of experience. The project is interesting perhaps a little too broad. Each group makes its own contribution. It would be nice to have more relation between the different groups…

OUTLINE OF THE TALK

Previous works: my skills, what I can do and topics on which we can start a collaboration (see latest work with Lecce, Pavia and Orsay)

Future works: what I plan to do (a chance for future collaborations?)

Recent calculations: pairing from two- and three-body forces in finite nuclei/
ground-state properties from mean-field approaches

PREVIOUS WORKS

PARITY VIOLATING ELECTRON SCATTERING

Electron - Nucleus Potential

$$\hat{V}(r) = V(r) + \gamma_5 A(r)$$

electromagnetic

$$V(r) = \int d^3 r' \; Z \rho(r') / |\vec{r} - \vec{r}'|$$

$$\frac{d\sigma}{d\Omega} = \frac{d\sigma}{d\Omega}_{Mott} \; |F_P(Q^2)|^2$$

axial

$$A(r) = \frac{G_F}{2\sqrt{2}} \left[(1 - 4\sin^2\theta_W) Z \rho_P(r) - N \rho_N(r) \right]$$

⇨ $A(r)$ is small, best observed by parity violation

⇨ $1 - 4\sin^2\theta_W << 1$ neutron weak charge >> proton weak charge

Proton form factor

$$F_P(Q^2) = \frac{1}{4\pi} \int d^3 r \; j_0(qr) \; \rho_P(r)$$

Neutron form factor

$$F_N(Q^2) = \frac{1}{4\pi} \int d^3 r \; j_0(qr) \; \rho_N(r)$$

Parity Violating Asymmetry

$$A = \frac{\left(\frac{d\sigma}{d\Omega}\right)_R - \left(\frac{d\sigma}{d\Omega}\right)_L}{\left(\frac{d\sigma}{d\Omega}\right)_R + \left(\frac{d\sigma}{d\Omega}\right)_L} = \frac{G_F Q^2}{2\pi\alpha\sqrt{2}} \left[\underbrace{1 - 4\sin^2\theta_W} - \frac{F_N(Q^2)}{F_P(Q^2)} \right]$$

from Urciuoli, PREX workshop@Trento 2009

PREVIOUS WORKS

PARITY VIOLATING ELECTRON SCATTERING

^{208}Pb experimental values (E=1 GeV and Θ=5°)
(Michaels, PAVI workshop 2011, submitted to PRL?)

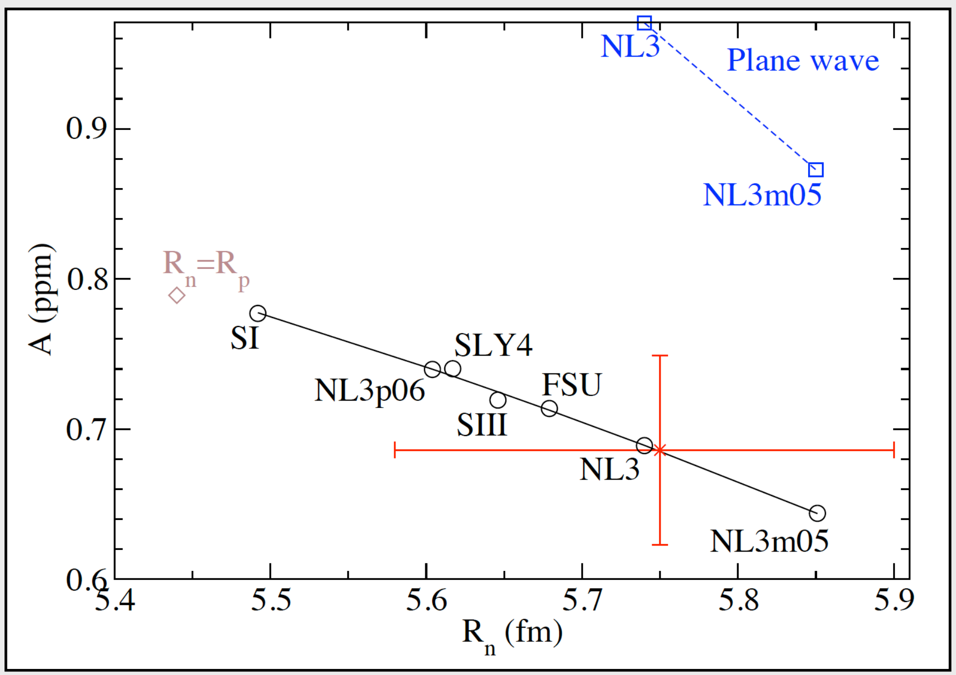

Theoretical calculations for tin isotopes

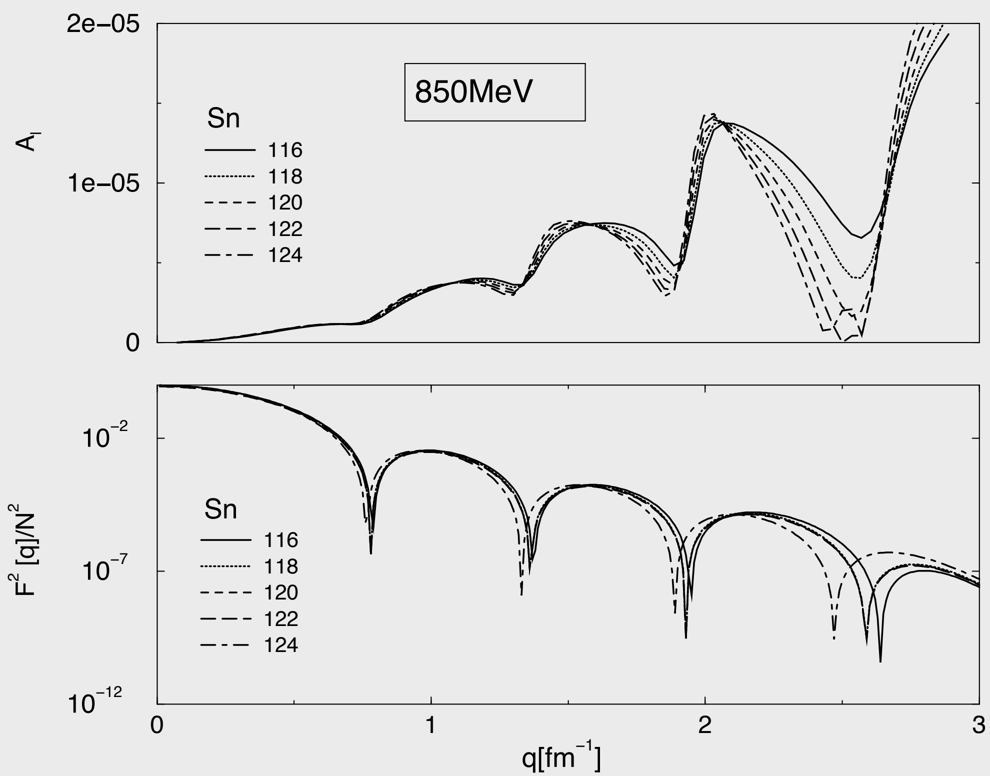

PREVIOUS WORKS

RELATIVISTIC MEAN FIELD MODELS
GROUND STATE PROPERTIES (RHB IN OPEN SHELL NUCLEI)

Meson-exchange

- non linear
- density dependent

Point coupling

- linear
- density dependent
  - phenomenological
  - chiral dynamics inspired

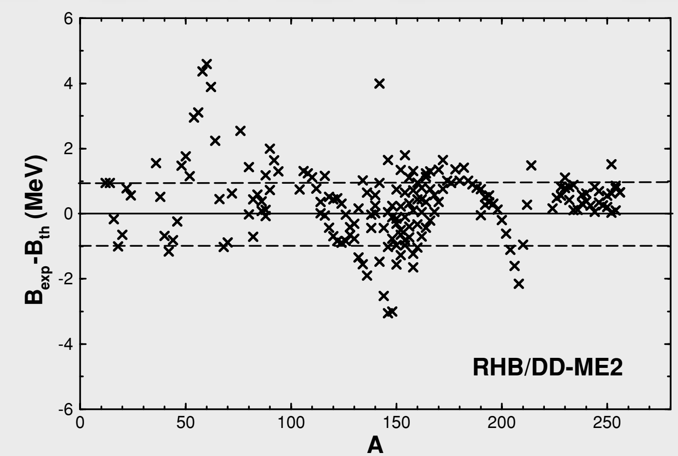

FIG. 2. Absolute deviations of the binding energies calculated with the DD-ME2 interaction from the experimental values [17].

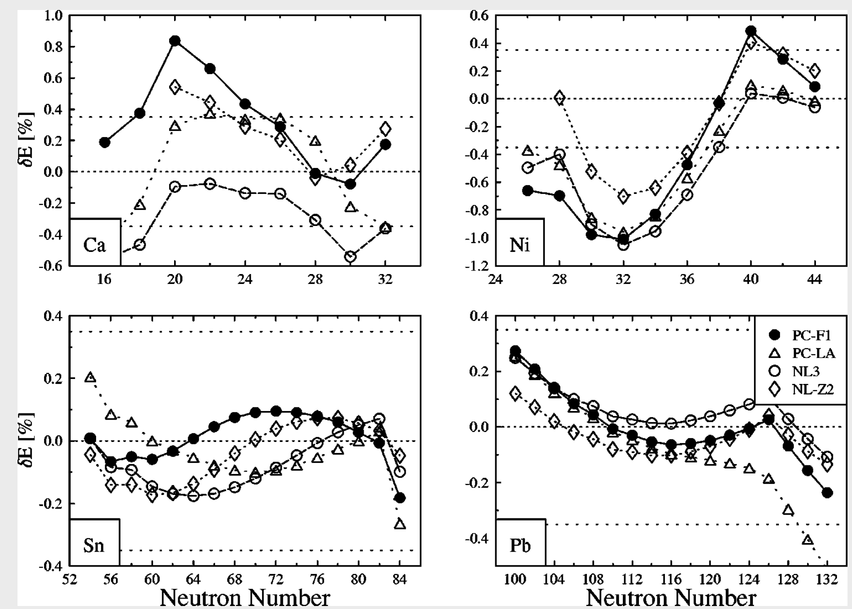

PREVIOUS WORKS

RELATIVISTIC MEAN FIELD MODELS
EXCITED STATE PROPERTIES (QRPA IN OPEN SHELL NUCLEI)

Meson-exchange

- non linear
- density dependent

Point coupling

- linear
- density dependent
  - phenomenological
  - chiral dynamics inspired

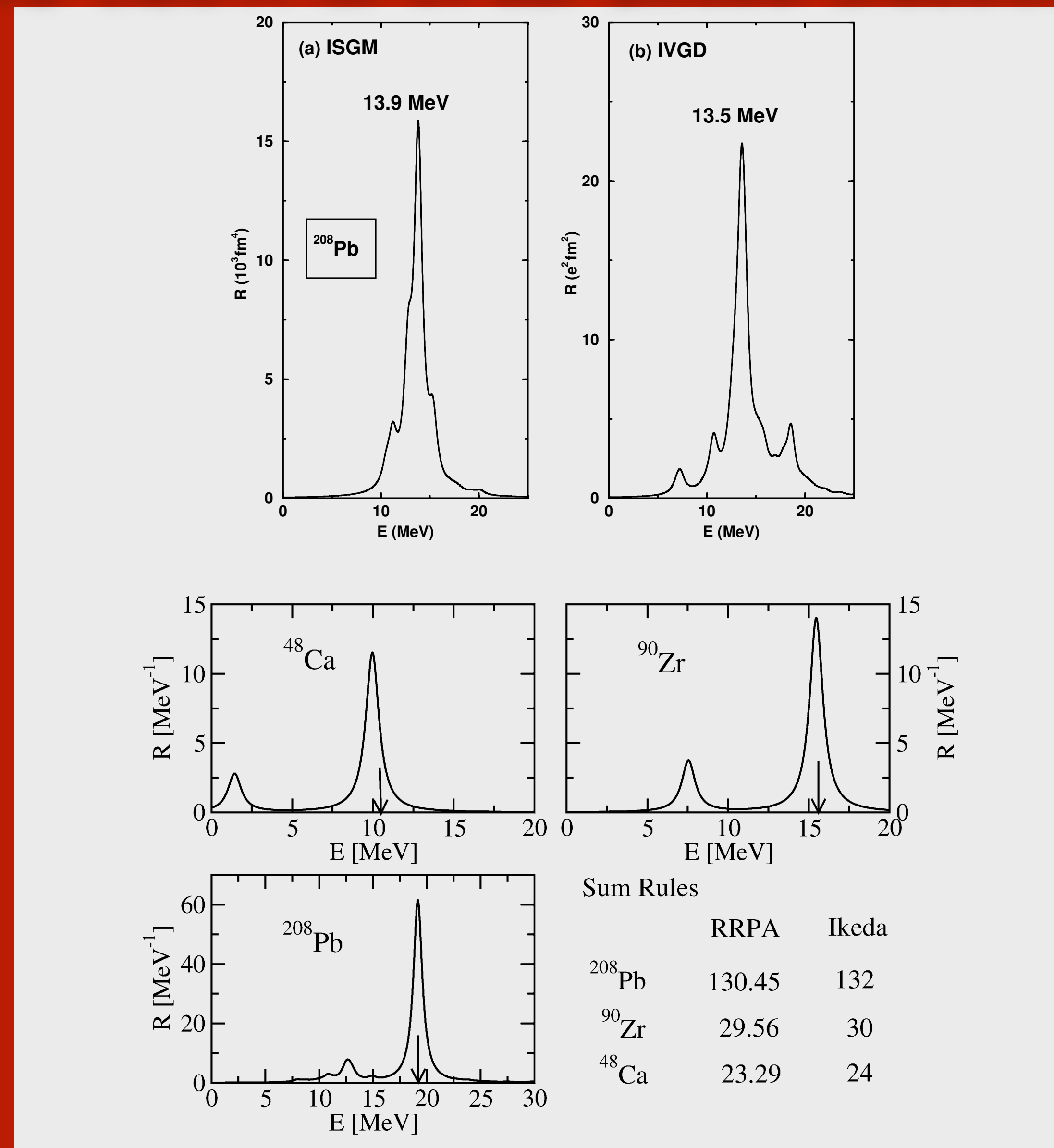

Previous Works

Hypernuclei
Vanishing Spin-Orbit Splittings

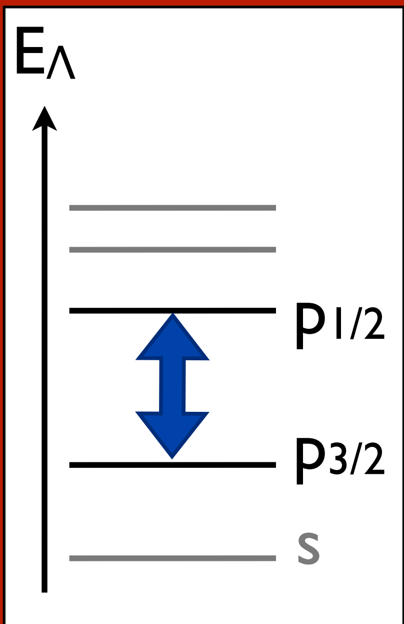

Table 4

P-shell spin–orbit splittings $\Delta \equiv \Delta\epsilon^{\Lambda}(p)$ for six hypernuclei ($^{13}_{\Lambda}$C, $^{16}_{\Lambda}$O, $^{40}_{\Lambda}$Ca, $^{89}_{\Lambda}$Y, $^{139}_{\Lambda}$La, $^{208}_{\Lambda}$Pb). Experimental values [44], or empirical estimates [1,47,48], are shown in comparison with our theoretical predictions (FKVW), using a broad range of ζ parameters (see Eq. (12)), and other relativistic calculations with (RMFI [11]) or without (RMFII [14]) tensor coupling. All energies are given in keV. The asterisk means that a local fit has been necessary.

Nucleus	Exp. Δ [keV]	FKVW $(0.4 \leqslant \zeta \leqslant 0.66)$	RMFI [11]	RMFII [14]
$^{13}_{\Lambda}$C	$152 \pm 54 \pm 36$ [44]	$-160 \leqslant \Delta \leqslant 510$	310	$\sim 1100^*$
$^{16}_{\Lambda}$O	$300 \leqslant \Delta \leqslant 600$ [47] $-800 \leqslant \Delta \leqslant 200$ [1]	$-210 \leqslant \Delta \leqslant 490$	270	~ 1400
$^{40}_{\Lambda}$Ca	–	$-140 \leqslant \Delta \leqslant 420$	210	~ 1400
$^{89}_{\Lambda}$Y	90 [48]	$-40 \leqslant \Delta \leqslant 180$	110	~ 700
$^{139}_{\Lambda}$La	–	$-20 \leqslant \Delta \leqslant 80$	50	~ 300
$^{208}_{\Lambda}$Pb	–	$-20 \leqslant \Delta \leqslant 70$	50	~ 300

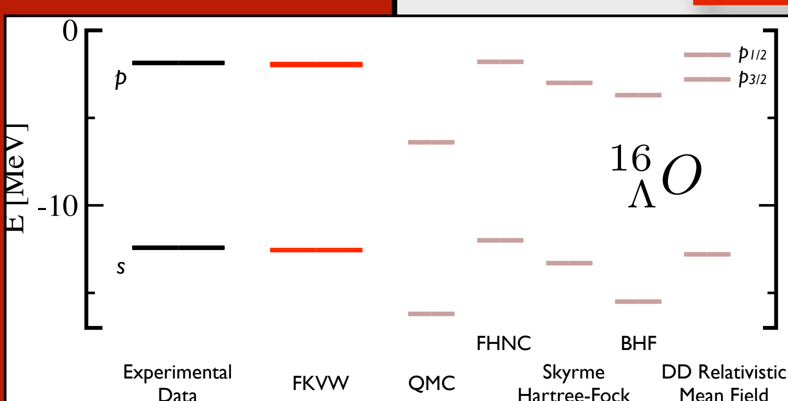

FUTURE WORKS

PARTICLE-VIBRATION COUPLING

Particle-vibration coupling is still an open issue: so far no theoretical approach is self-consistent

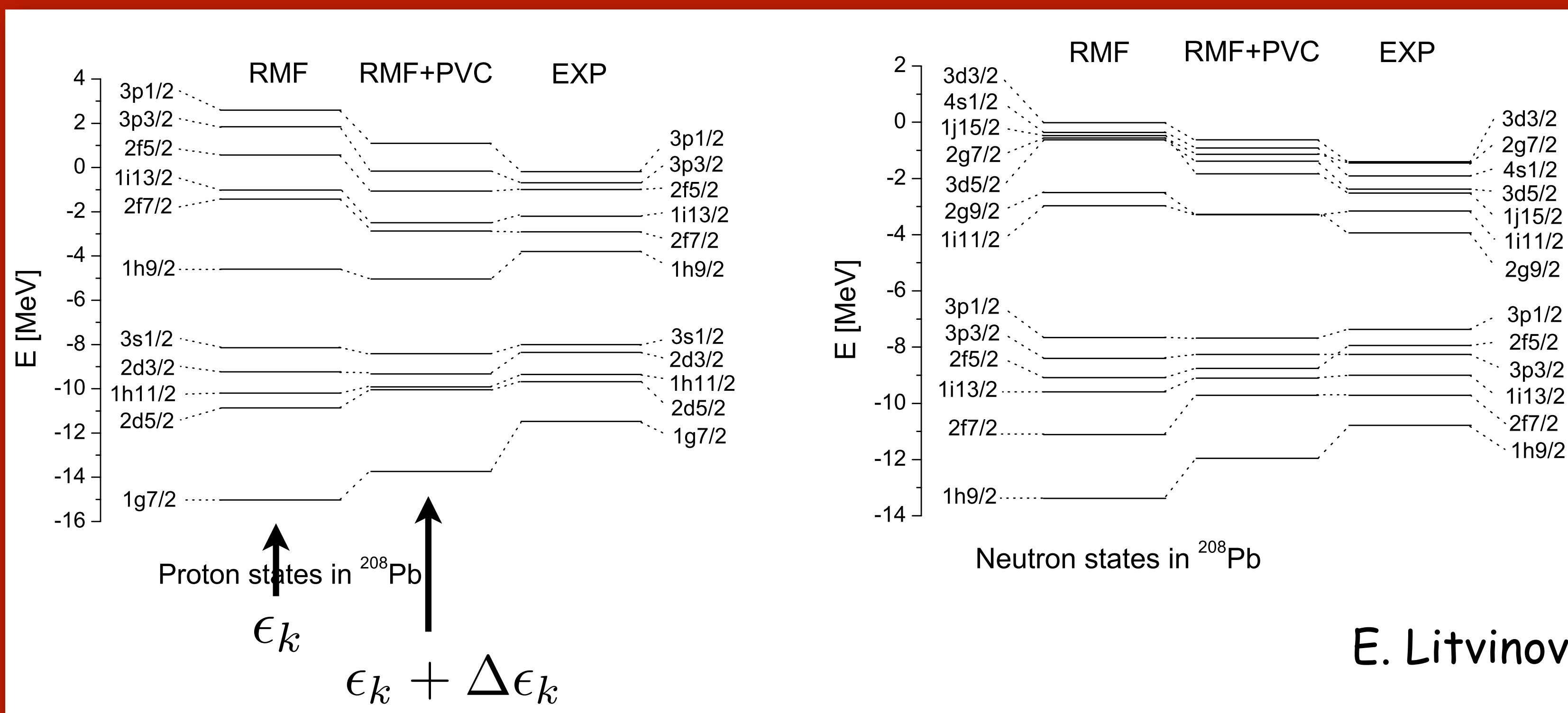

E. Litvinova et al.

Corrections are always on top of the mean-field calculation

FUTURE WORKS

PARTICLE-VIBRATION COUPLING: OPM?

In this approach E_{xc} is expressed in terms of the KS orbitals and eigenvalues rather than density itself

$$\left[-\frac{\nabla^2}{2m}+v_s(\boldsymbol{r})\right]\phi_k(\boldsymbol{r})=\epsilon_k\phi_k(\boldsymbol{r})$$

KS potentials

$$\begin{aligned} v_s(\boldsymbol{r}) &= v_{\rm ext}(\boldsymbol{r})+v_{\rm H}(\boldsymbol{r})+v_{\rm xc}(\boldsymbol{r}) \\ v_{\rm H}(\boldsymbol{r}) &= e^2\int {\rm d}^3r'\,\frac{n(\boldsymbol{r}')}{|\boldsymbol{r}-\boldsymbol{r}'|} \\ v_{\rm xc}(\boldsymbol{r}) &= \frac{\delta E_{\rm xc}[n]}{\delta n(\boldsymbol{r})}\,. \end{aligned}$$

Density

$$n(\boldsymbol{r})=\sum_k \Theta_k|\phi_k(\boldsymbol{r})|^2$$

Total energy

$$E_{\rm tot}[n]=T_s[n]+E_{\rm ext}[n]+E_{\rm H}[n]+E_{\rm xc}[n]\ \Big(+E_{\rm ion}\Big)$$

Kinetic term

External potential

Hartree potential

Exchange correlation term

FUTURE WORKS

PARTICLE-VIBRATION COUPLING: OPM?

External potential

$$E_{\rm ext}[n] = \int \mathrm{d}^3r\, v_{\rm ext}(\boldsymbol{r}) n(\boldsymbol{r})$$

Hartree potential

$$E_{\rm H}[n] = \frac{e^2}{2} \int \mathrm{d}^3r \int \mathrm{d}^3r' \, \frac{n(\boldsymbol{r})\, n(\boldsymbol{r}')}{|\boldsymbol{r} - \boldsymbol{r}'|}$$

Exchange correlation term

Explicit dependence on KS orbitals and energies

$$\frac{\delta E_{\rm xc}[\phi_k, \epsilon_k]}{\delta n(\boldsymbol{r})} = \int \mathrm{d}^3r' \, \frac{\delta v_{\rm s}(\boldsymbol{r}')}{\delta n(\boldsymbol{r})} \sum_k \left\{ \int \mathrm{d}^3r'' \left[\frac{\delta \phi_k^\dagger(\boldsymbol{r}'')}{\delta v_{\rm s}(\boldsymbol{r}')} \frac{\delta E_{\rm xc}}{\delta \phi_k^\dagger(\boldsymbol{r}'')} + c.c. \right] + \frac{\delta \epsilon_k}{\delta v_{\rm s}(\boldsymbol{r}')} \frac{\partial E_{\rm xc}}{\partial \epsilon_k} \right\} \quad (2$$

FUTURE WORKS

CORRELATIONS IN MEAN FIELD MODELS

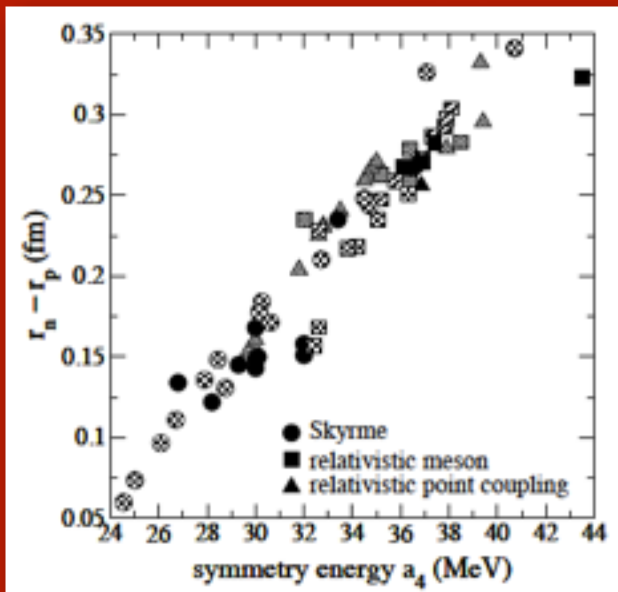

Correlations between different "observables" for several relativistic and non-relativistic functionals

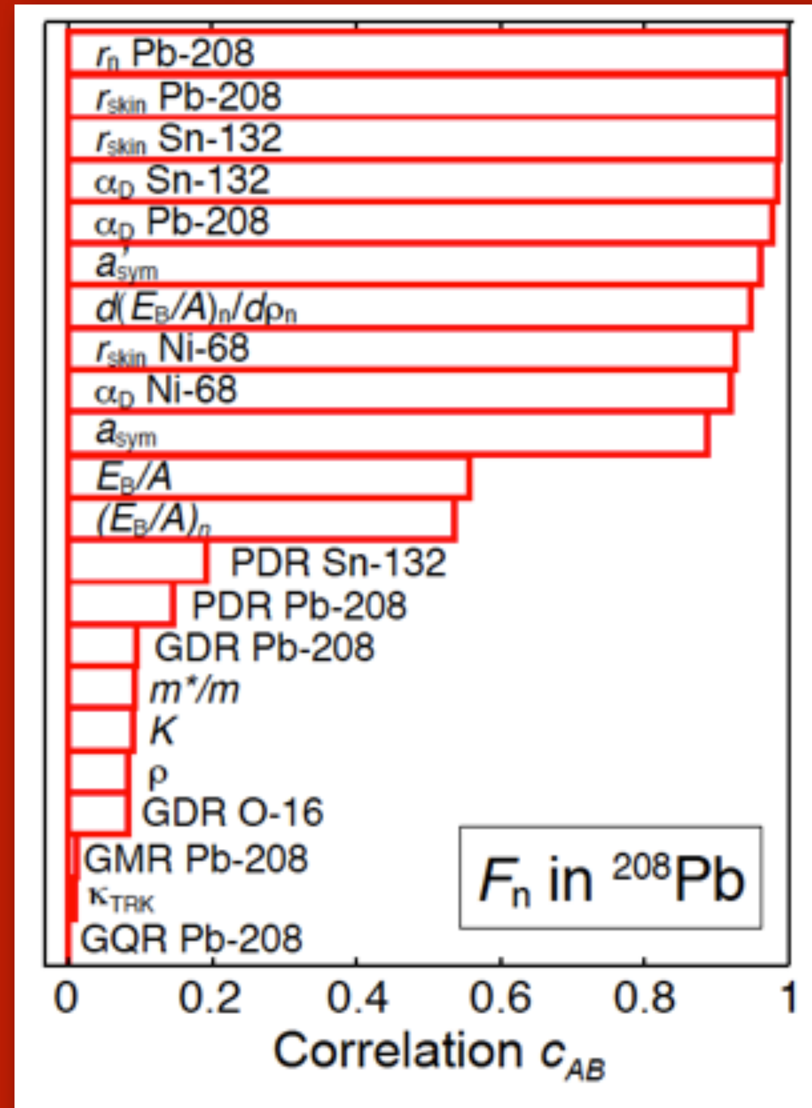

FIG. 2: (Color online) Correlation (6) of various observables with the neutron form factor $F_n(q=0.45\,\text{fm}^{-1})$ in ^{208}Pb.

Correlations between nuclear matter and finite nuclei "observables"

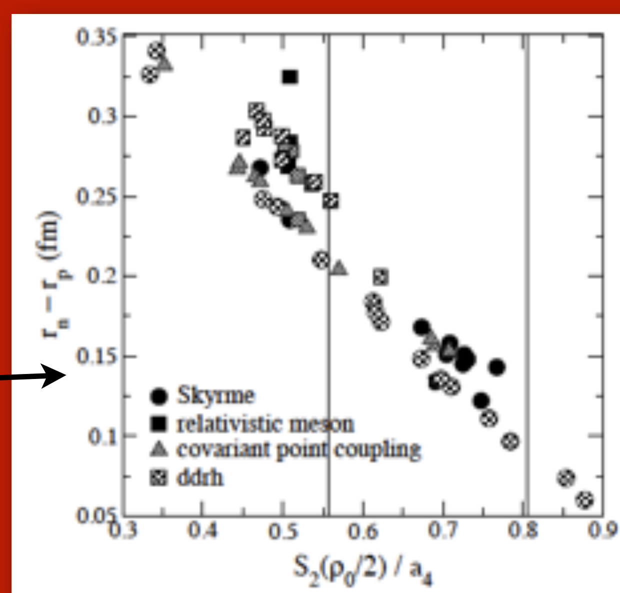

FUTURE WORKS

NON-RELATIVISTIC ENERGY DENSITY FUNCTIONAL FROM CHIRAL DYNAMICS

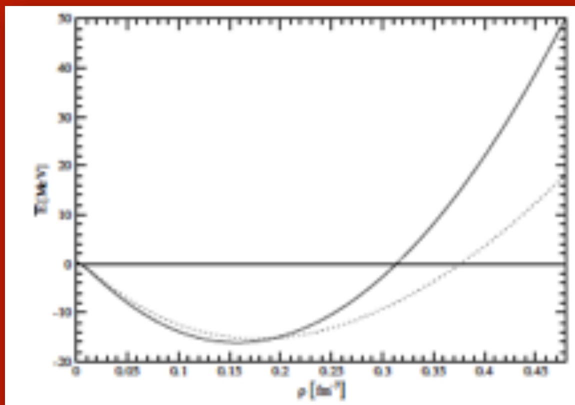

Energy per particle

Effective mass

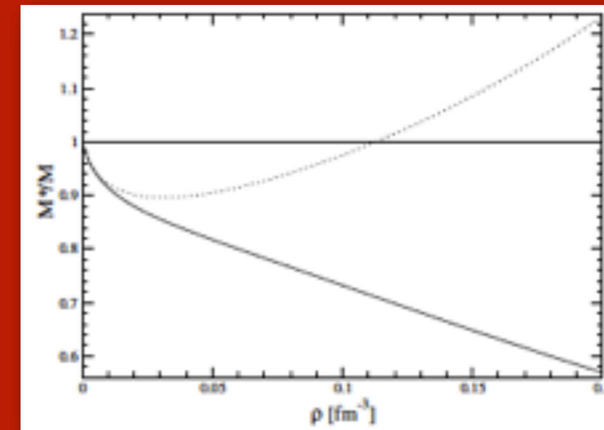

$$\mathcal{E}[\rho,\tau,\mathbf{J}] = \rho\,\bar{E}(k_f) + \left[\tau - \frac{3}{5}\rho k_f^2\right]\left[\frac{1}{2M_N} - \frac{5k_f^2}{56M_N^3} + F_\tau(k_f)\right] + (\nabla\rho)^2 F_\nabla(k_f) + \nabla\rho\cdot\mathbf{J}\,F_{so}(k_f) + \mathbf{J}^2 F_J(k_f)$$

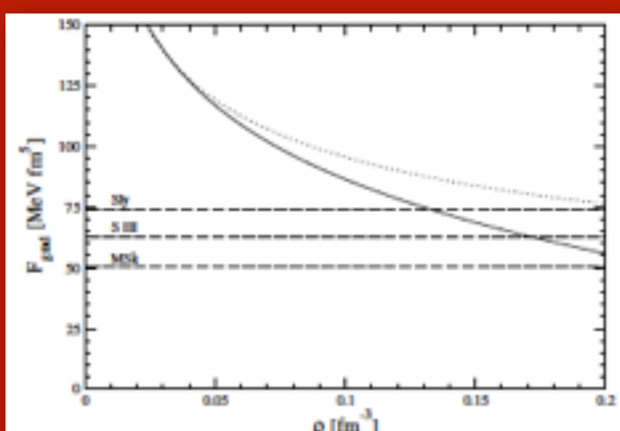

Gradient function

Spin-orbit function

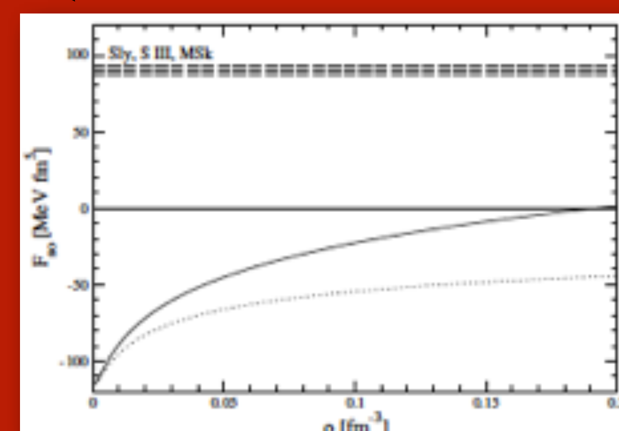

LATEST WORKS

APPLICATIONS OF IN-MEDIUM CHIRAL DYNAMICS TO NUCLEAR STRUCTURE:

A REALISTIC PAIRING INTERACTION

(NUCL-TH/1111.4946, SUBMITTED TO PRC)

With D. Vretenar and T. Niksic (University of Zagreb); Many thanks to N. Kaiser, W. Weise and J. Holt (Technical University of Munich) for numerical results.

INTRODUCTION

- Keep things as simple as possible: find a fast and computationally efficient way to include a **realistic** pairing in HFB calculations (of course, using explicit formulas is not an option).

realistic? 2-body plus 3-body (with some approximations)

- Solve the gap equation for symmetric nuclear matter.

- Use a parametrized pairing force that, on one hand, reproduces the realistic pairing gap in symmetric nuclear matter and, on the other hand, is easy to use for finite systems. Try to include all the physical informations. Not only the pairing gap at some Fermi momentum, but all k_F-dependence: fix parameters in order to reproduce $\Delta(k_F)$.

- Test the realistic potential in finite nuclei: pairing gaps in isotopic and isotonic chains.

THE GAP EQUATION

V: pairing potential

Δ: pairing field

$$\Delta(k,k_F) = -\frac{1}{4\pi^2}\int_0^\infty \frac{p^2 V(p,k)\Delta(p,k_F)}{\sqrt{[\mathcal{E}(p,k_F)-\mathcal{E}(k_F,k_F)]^2+\Delta(p,k_F)^2}}\mathrm{d}p$$

ε: quasiparticle energy

ε_F: Fermi energy

$$\mathcal{E}(p,k_F)-\mathcal{E}(k_F,k_F) = \frac{p^2-k_F^2}{2M^*(k_F)}$$

$V(p,k) = V_{2B}(p,k) + V_{3B}(k_F,p,k)$

- ☑ Two-body: **N3LO** by Machleidt & Entem [Phys. Rep. **503** (2011) 1].
- ☑ Three-body: **effective two-body density-dependent interaction** developed by Holt, Kaiser and Weise [PRC **81** (2010) 024002]. See also Hebeler et al. [PRC **82** (2010) 014314 and nucl-th/1104.2955].

- ☑ For the energies we could use the bare mass (M_N) but it would be better to use an **effective mass (M*)** [Fritsch, Kaiser and Weise, NPA **750** (2005) 259 or Holt, Kaiser and Weise, nucl-th/1107.5966].

2-BODY INTERACTION (N3LO)

R. Machleidt, D.R. Entem / Physics Reports 503 (2011) 1–75

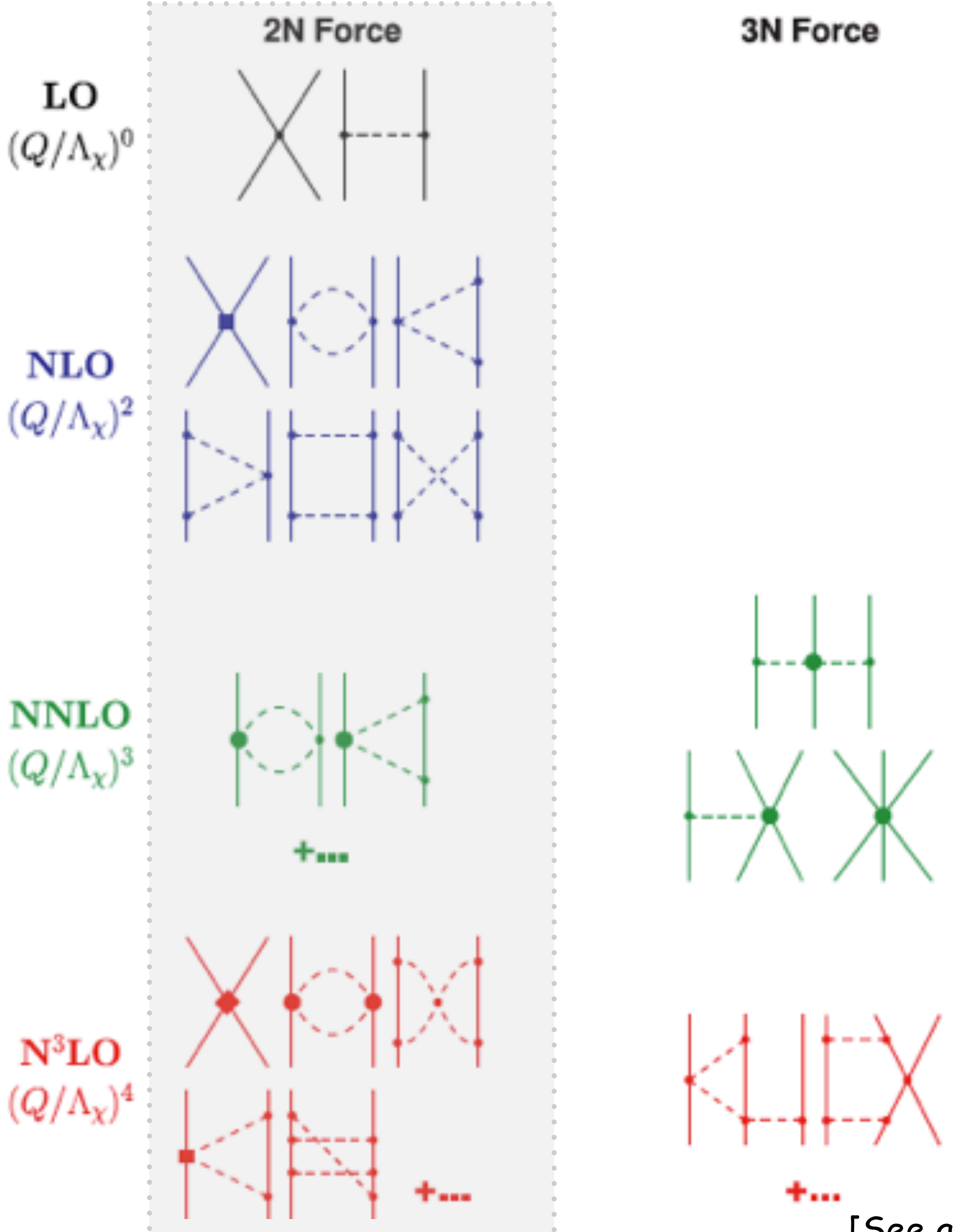

Phase shifts of np scattering as calculated from NN potentials at different orders of ChPT

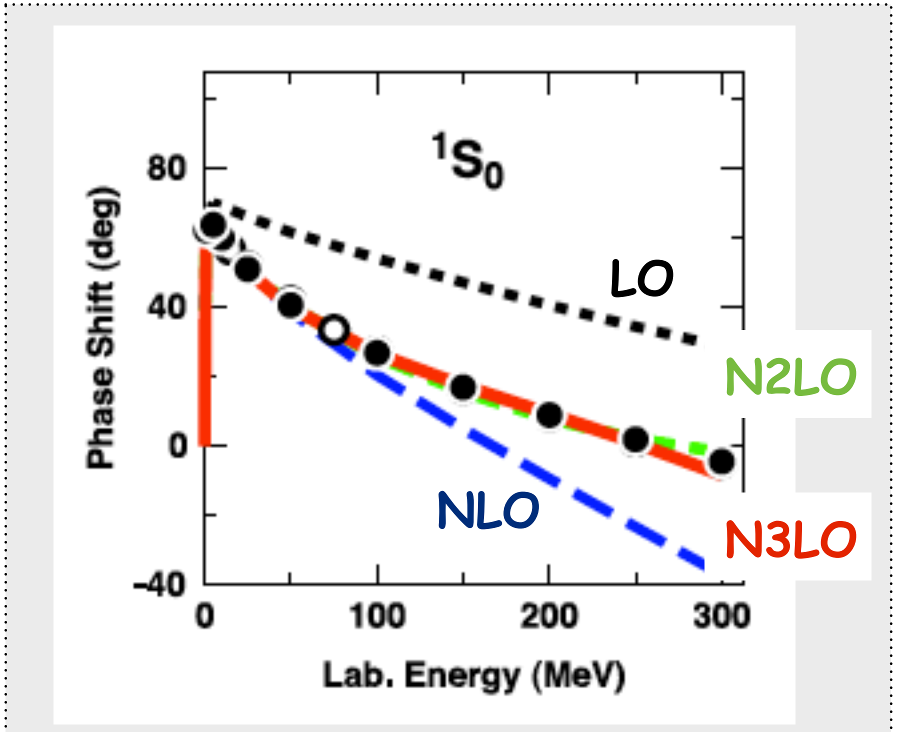

(black dots are experimental data)

[See also Epelbaum, Hammer and Meissner, RMP **81** (2009) 1773]

Results from N3LO (with bare mass)

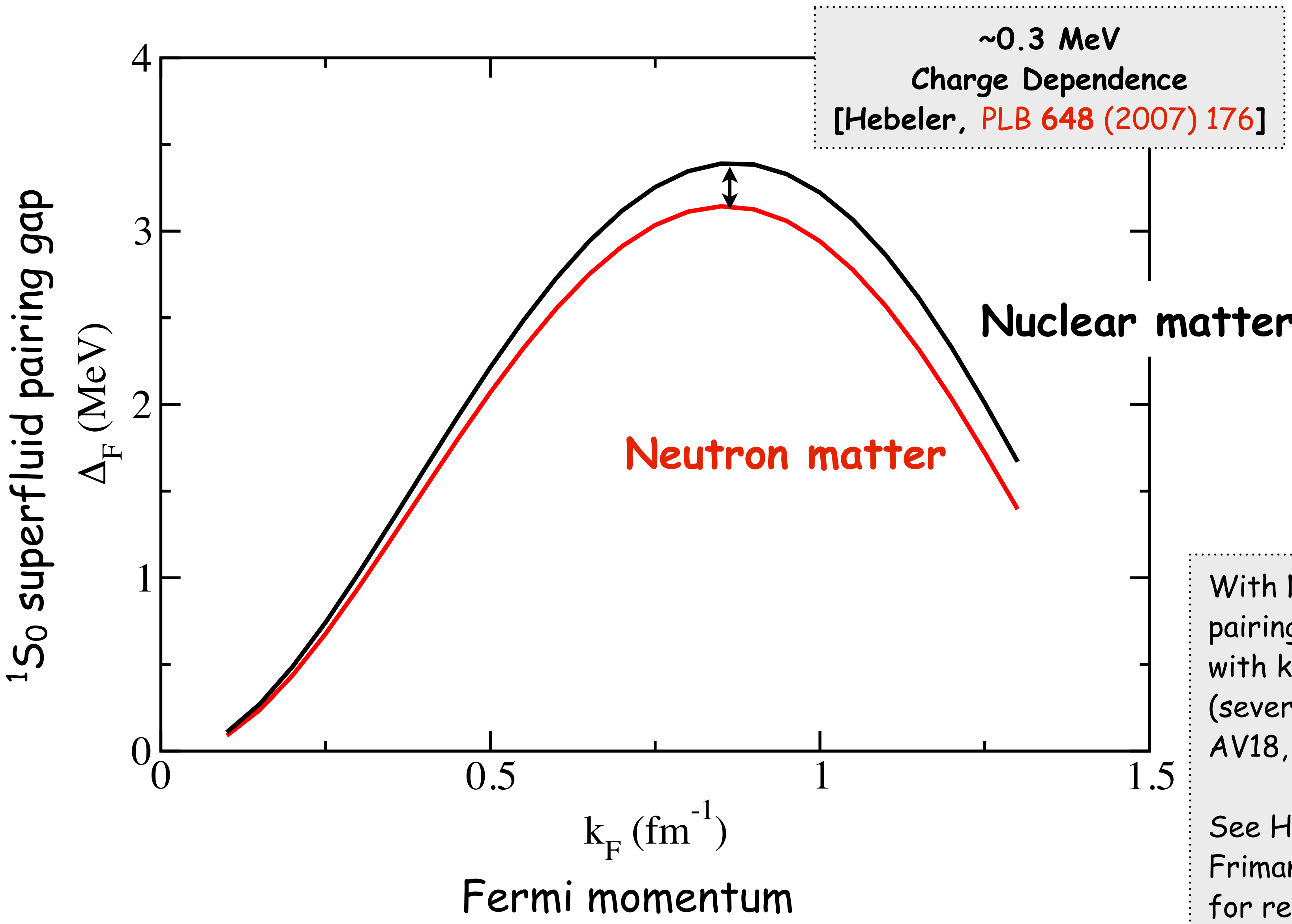

With N3LO interaction, pairing gaps in good agreement with known calculations (several realistic interactions: AV18, CD-Bonn, Nijmegen,...).

See Hebeler, Schwenk and Friman, PLB **648** (2007) 176 for recent V_{lowk} calculations.

EFFECTIVE MASS M*

Holt, Kaiser and Weise, nucl-th/1107.5966

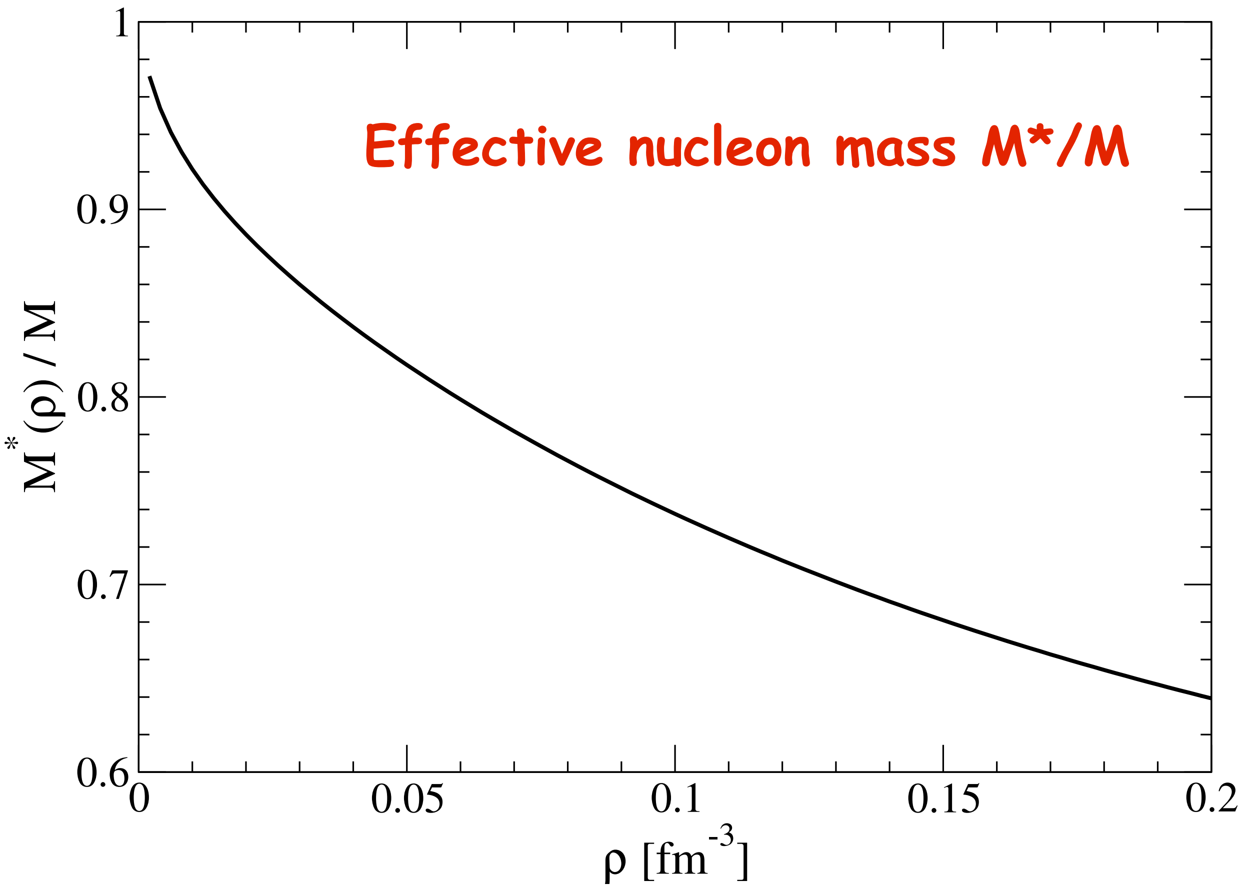

Substantial agreement with non relativistic Skyrme phenomenology at saturation density ($0.7 < M^*/M < 1$).

The two-body interaction includes long-range one- and two-pion exchange contributions and a set of contact terms contributing up to fourth power in momenta.

In addition they add the leading order chiral 3N interaction with its parameters c_E, c_D and $c_{1,3,4}$.

RESULTS FROM N3LO (WITH M*)

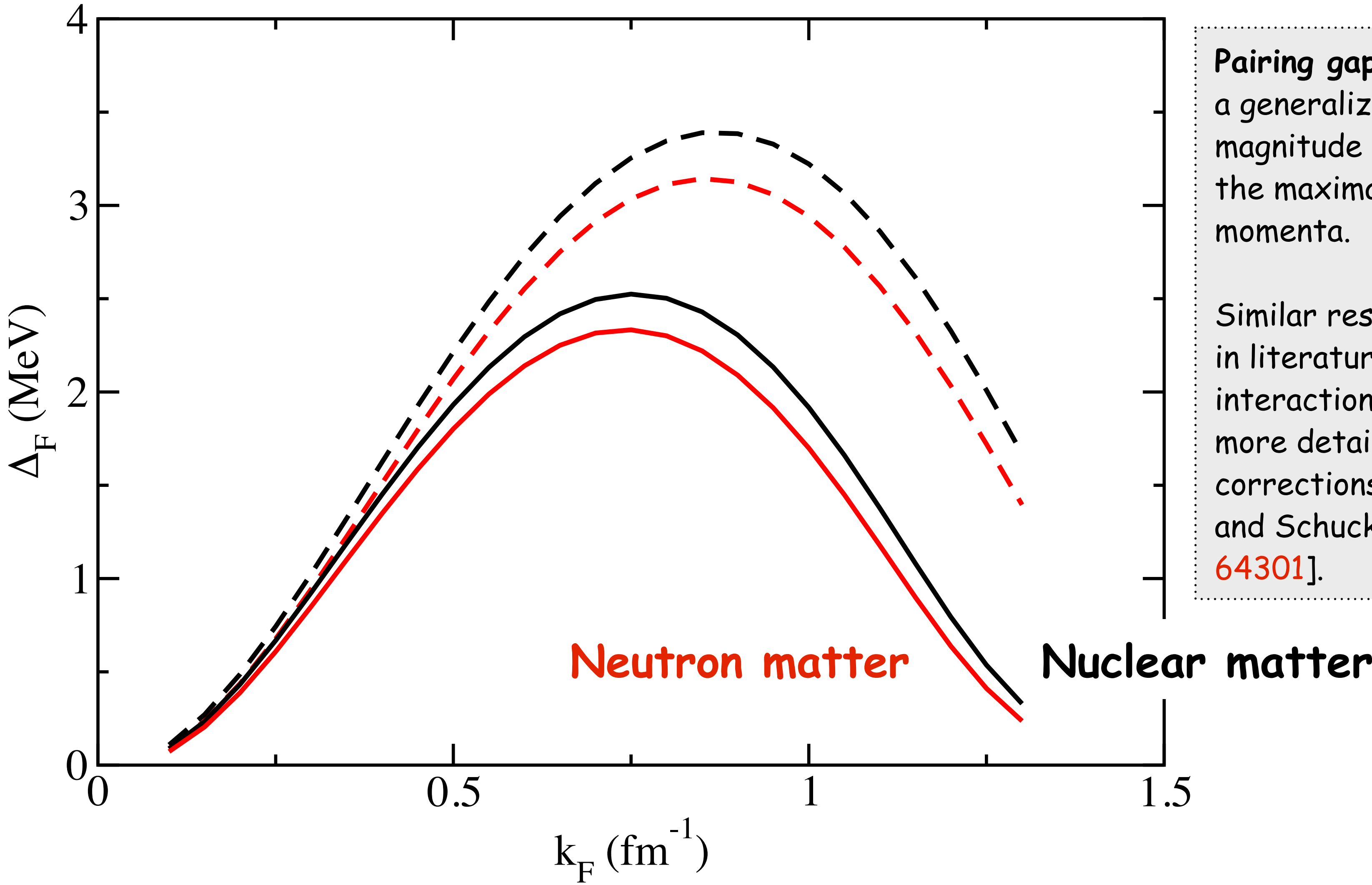

Fermi momentum

$^1S_0$ superfluid pairing gap

Pairing gaps are changed: a generalized reduction in magnitude and a small shift of the maxima towards smaller momenta.

Similar results are well-known in literature [with Gogny interaction, EPJA **25** (2005); more details about medium corrections in Cao, Lombardo and Schuck, PRC **74** (2006) 64301].

Effective masses from Holt et al., **1107.5966**

3-BODY INTERACTION

R. Machleidt, D.R. Entem / Physics Reports 503 (2011) 1–75

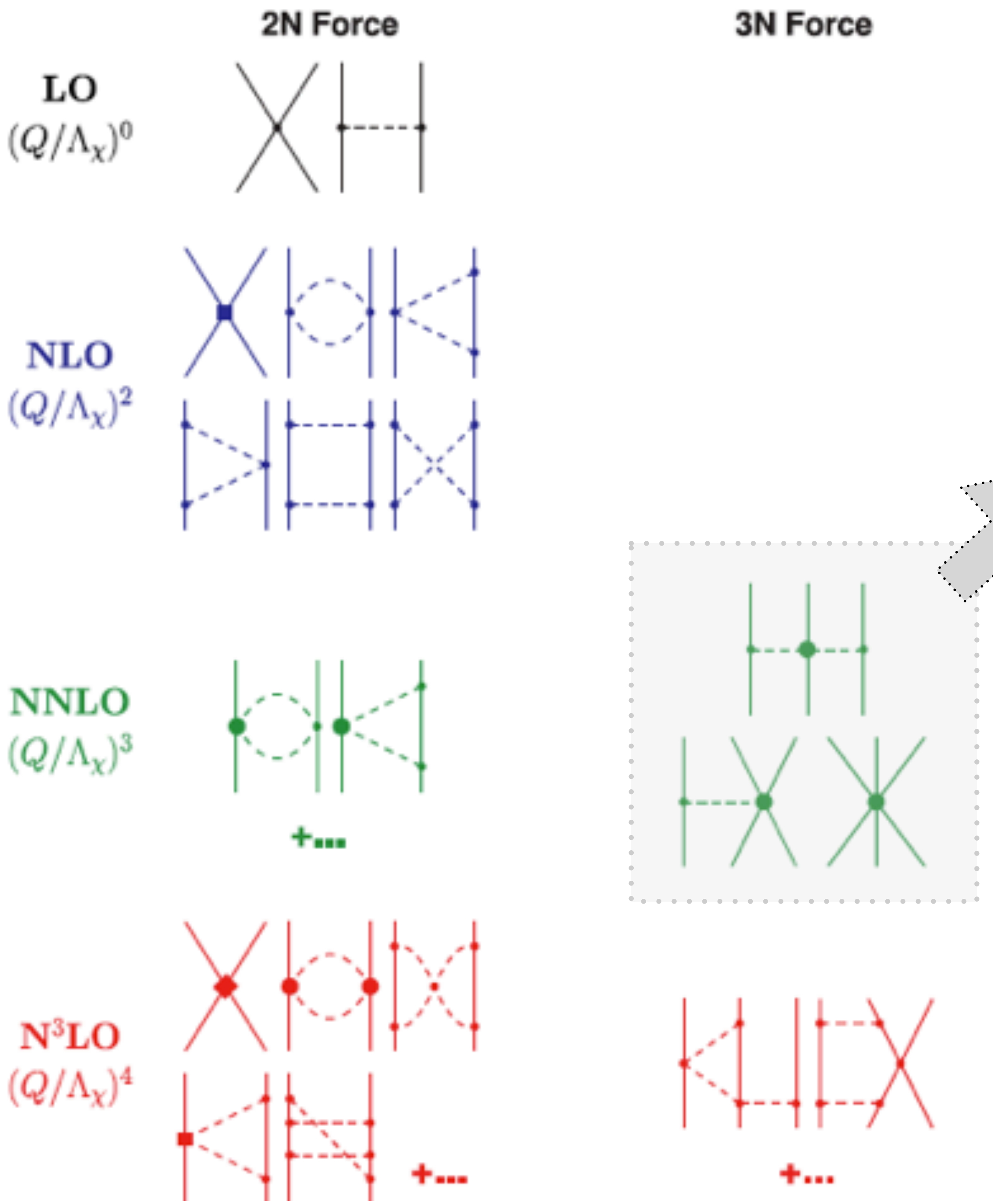

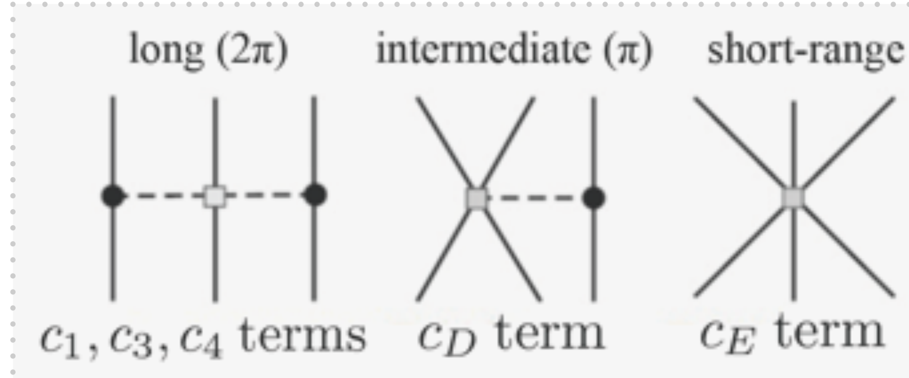

$$c_1 = -0.9^{+0.2}_{-0.5}\,,\quad c_3 = -4.7^{+1.5}_{-1.0}\,,\quad c_4 = 3.5^{+0.5}_{-0.2}$$

- ☑ c_i known from π**N** scattering
- ☑ c_D and c_E fixed from binding energies of light nuclei (^{3}He, ^{4}He) and/or **nd** scattering length

3-BODY INTERACTION

R. Machleidt, D.R. Entem / Physics Reports 503 (2011) 1–75

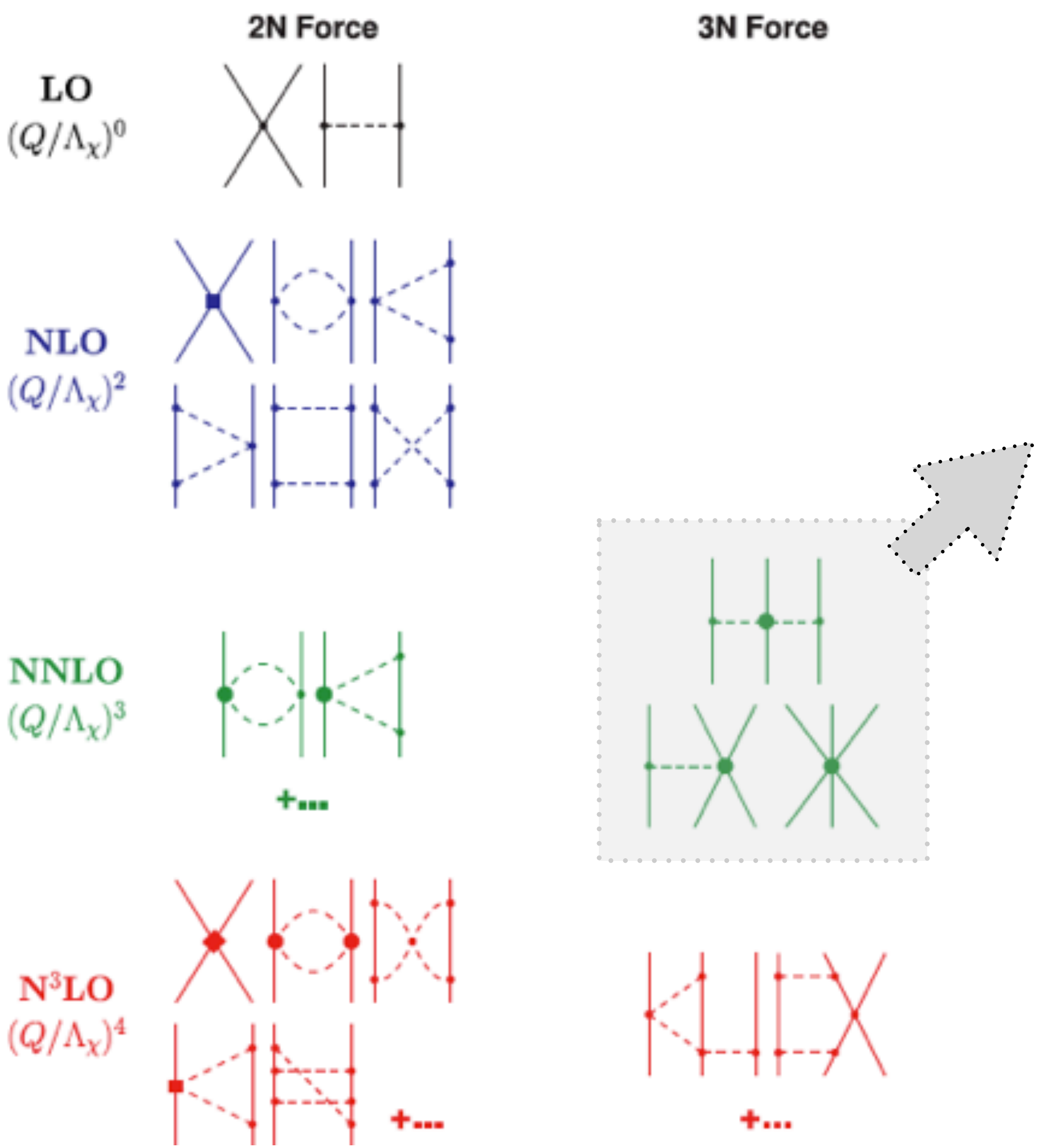

3 body ➜ 2 body density dependent

Holt et al., [PRC **81** (2010) 024002]

In-medium NN interaction generated by the two-pion exchange component (c_1,c_3,c_4) of the chiral three-nucleon interaction.

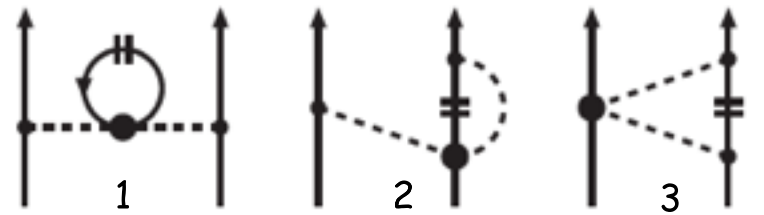

In-medium NN interaction generated by the one-pion exchange (c_D) and short-range component (c_E) of the chiral three-nucleon interaction.

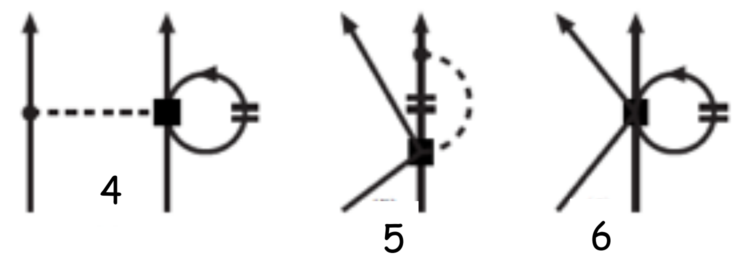

in-medium nucleon propagator $-2\pi\delta(k_0)\,\theta(k_f-|\vec{k}\,|)$

3-BODY INTERACTION

Holt et al., [PRC **81** (2010) 024002]

In-medium NN interaction generated by the two-pion exchange component (c_1,c_3,c_4) of the chiral three-nucleon interaction.

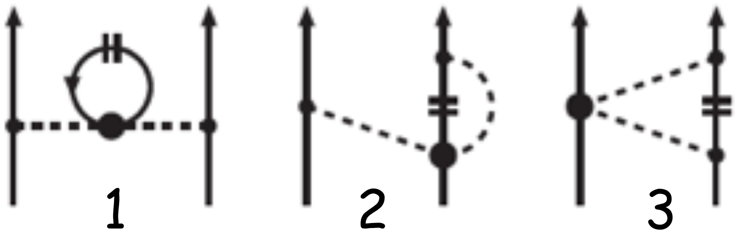

In-medium NN interaction generated by the one-pion exchange (c_D) and short-range component (c_E) of the chiral three-nucleon interaction.

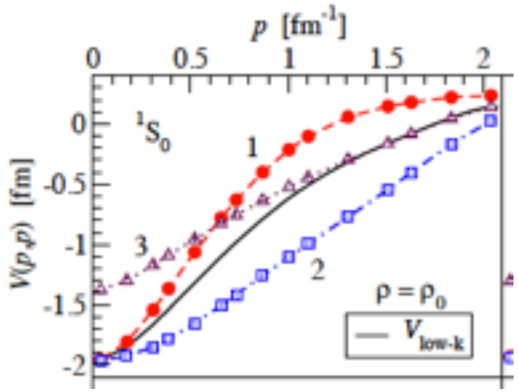

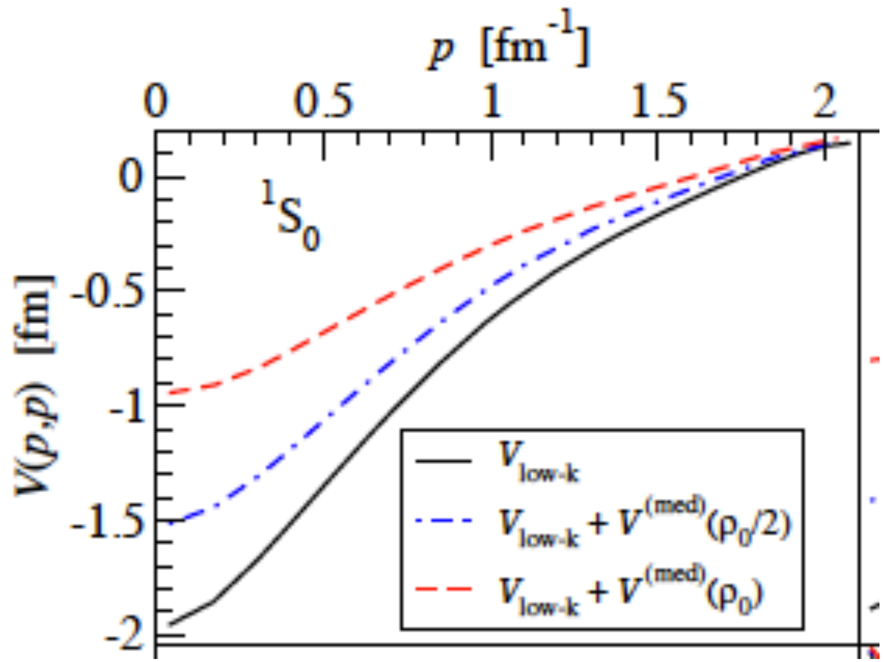

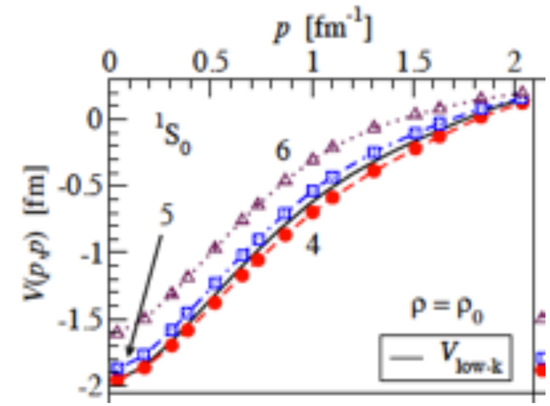

The attraction is reduced by the action of the three-body forces

RESULTS FROM 3-BODY

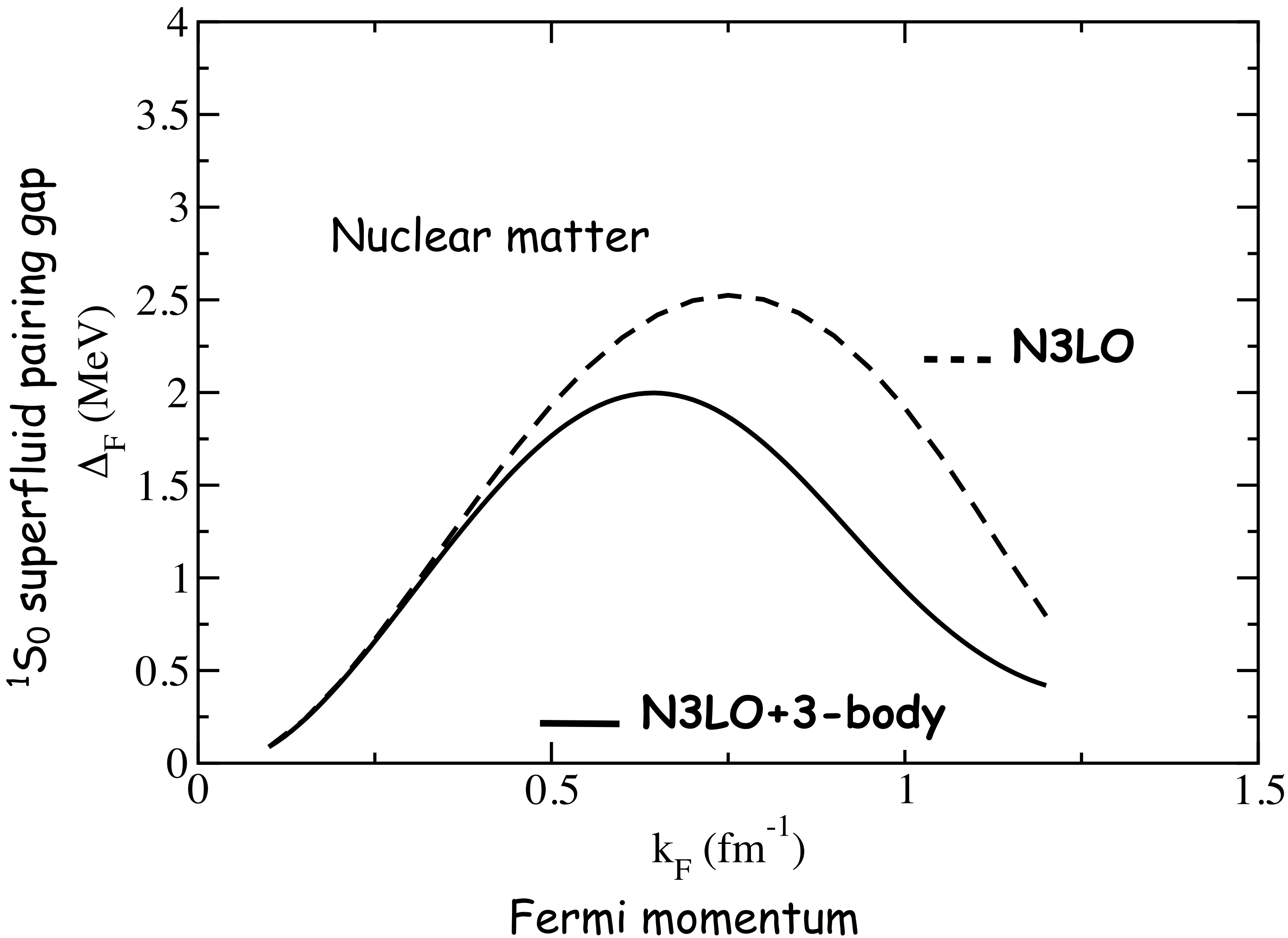

Pairing gaps are changed: a small reduction in magnitude and a relevant shift of the maximum towards smaller momenta.

Known calculations for pairing gaps with three-body forces included in the nuclear potential are: Hebeler and Schwenk, PRC **82** (2010) 014314; Zuo, Lombardo, Schulze and Shen, PRC **66** (2002) 037303.

Effective masses from Holt et al., **1107.5966**

NEUTRON MATTER WITH 2B AND 3B PRELIMINARY!

neutron matter

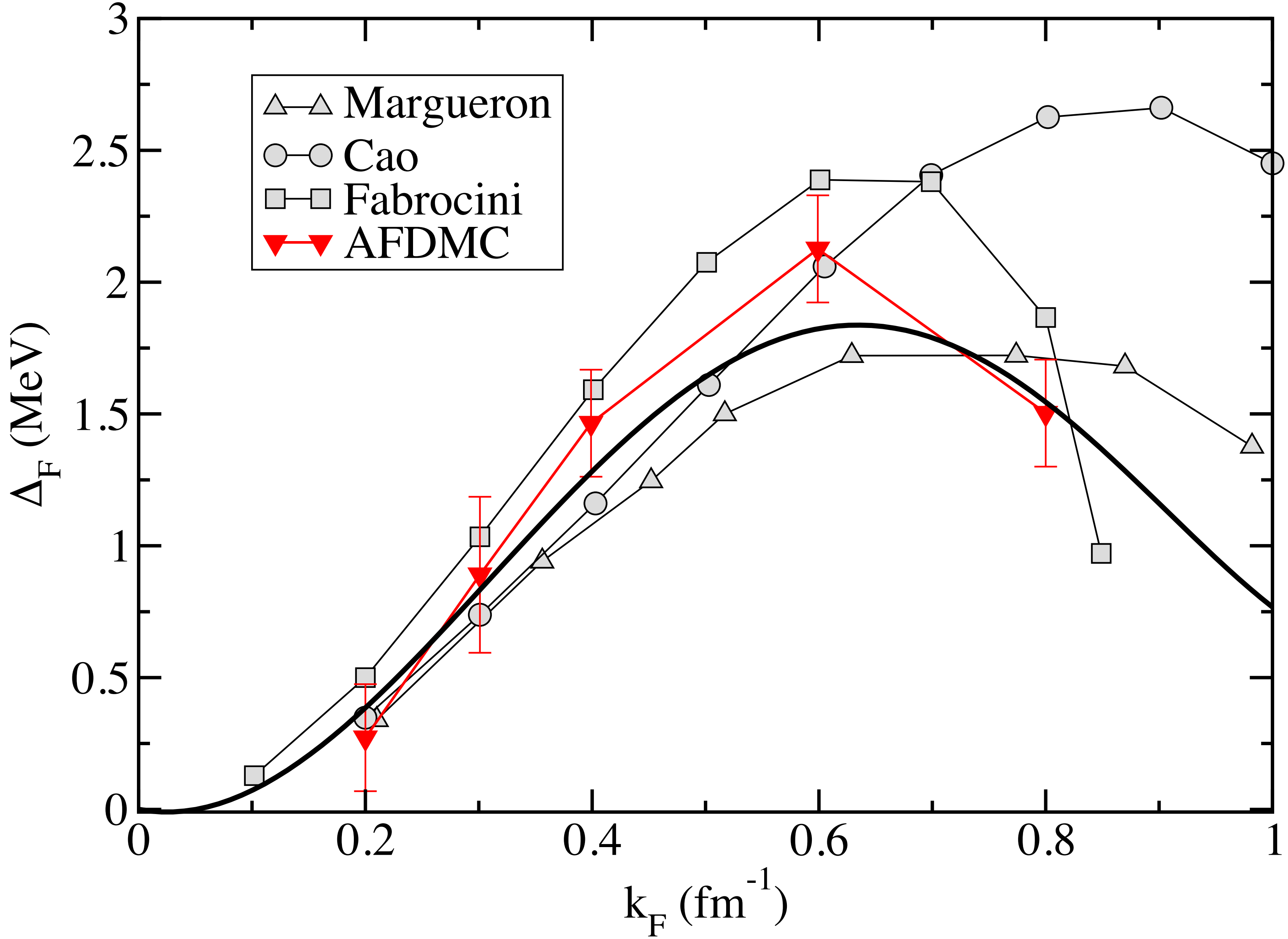

SEPARABLE PAIRING BY Y. TIAN

In nuclear matter the pairing interaction has a separable form in momentum space

$$\langle \boldsymbol{k} | V^{^1S_0} | \boldsymbol{k}' \rangle = -Gp(k)p(k')$$

Gaussian ansatz

$$p(k) = e^{-a^2k^2}$$

The two parameters **G** and **a** can be adjusted to reproduce the density dependence of the gap at the Fermi surface. The ansatz can be tested over well known calculations (like Gogny). Energies (pairing and binding) and gaps are reproduced with very high accuracy.

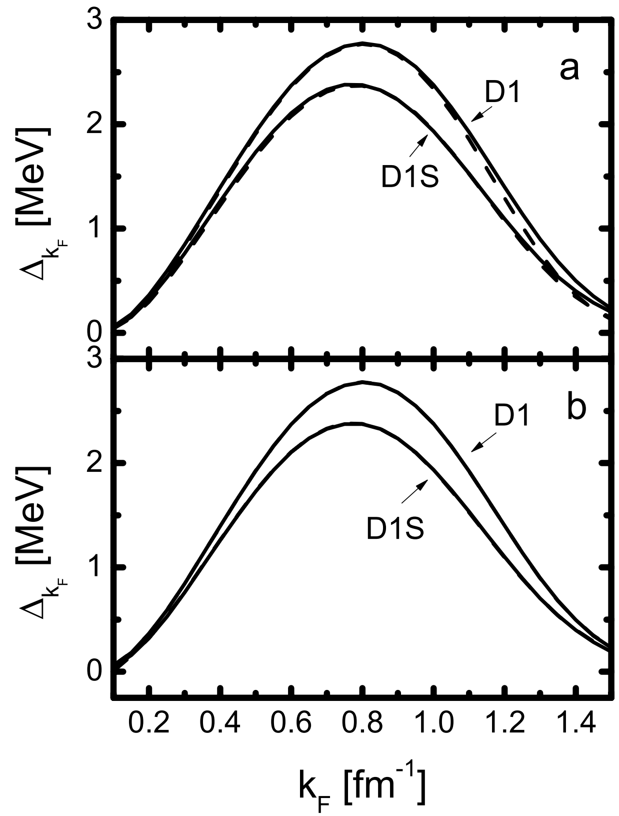

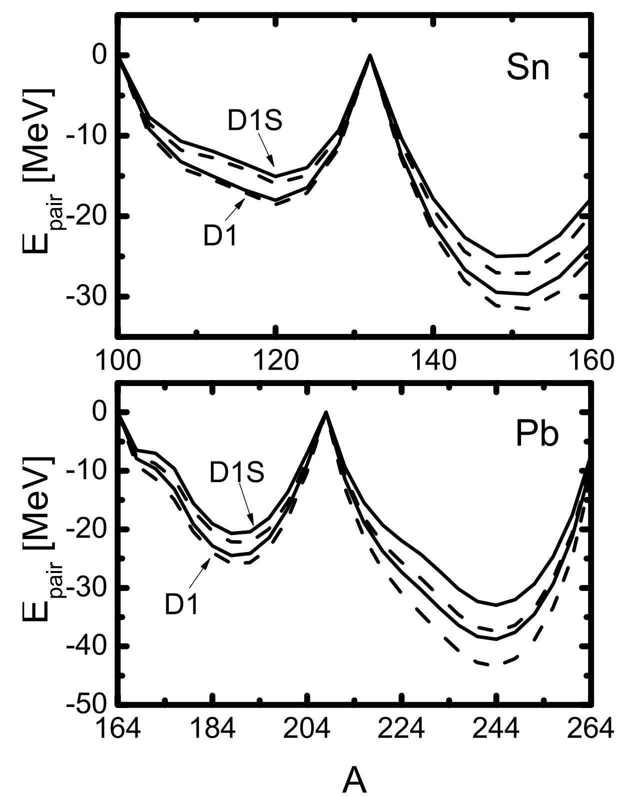

[Y. Tian et al., PLB **676** (2009) 44; Veselý, Dobaczewski, Michel and Toivanen, JoP Conf. Ser., **267** (2011) 012027]

FINITE NUCLEI CALCULATIONS

Δ: pairing field

$$\begin{pmatrix} h-\mu & \Delta \\ \Delta & -h+\mu \end{pmatrix} \begin{pmatrix} U \\ V \end{pmatrix}_k = E_k \begin{pmatrix} U \\ V \end{pmatrix}$$

In the hamiltonian **h** we have
V_{ph}: particle-hole potential

μ: chemical potential

Three possible choices for **V_{ph}**:

- ☑ **FKVW**: Density-dependent point coupling model constrained by in-medium chiral interactions, see Finelli et al. [NPA **770** (2006) 1] for ground-state calculations. Applications also for excited-state properties and, in particular, hypernuclei in the last years.
- ☑ **PC-F1**: Non-linear point coupling model, see Burvenich et al. [PRC **65** (2002) 044308]; see also Madland et al. [PRC **46** (1992) 1757] for the first application to finite nuclei.
- ☑ **PC-D1**: Density-dependent point coupling model, see Niksic et al. [PRC **78** (2008) 034318] and, for density-dependent theories, Typel et al. [NPA **656** (1999) 331].

PAIRING GAPS IN FINITE NUCLEI

Theory

State-dependent single-particle states

$$\bar{\Delta} = \frac{\sum_k \Delta_k v_k^2}{\sum_k v_k^2}$$

Occupation factors

Alternative choice

$$\bar{\Delta} = \frac{\sum_k \Delta_k v_k u_k}{\sum_k v_k u_k}$$

Δ_k are the diagonal matrix elements of the pairing part of the RHB single-nucleon hamiltonian in the canonical basis (the basis that diagonalizes the 1-particle density matrix)

[Lalazissis, Vretenar and Ring, PRC **57** (1997) 2294; Bender, Rutz, Reinhard and Maruhn, EPJA **8** (2000) 59]

Empirical Estimates

$$\Delta^{(5)}(N_0) = -\frac{1}{8}\left[E(N_0+2) - 4E(N_0+1) + 6E(N_0) - 4E(N_0-1) + E(N_0-2)\right]$$

Five-points formula

[Bender, Rutz, Reinhard and Maruhn, EPJA **8** (2000) 59]

Alternative approach

Theoretical gaps are provided by Δ_{LCS} (Lowest Canonical State) which denotes the diagonal pairing matrix element Δ_i corresponding to the canonical single-particle state Φ_i whose quasi-particle energy is the lowest.
Experimental gaps extracted from binding energies through three-point mass differences centered on odd-mass nuclei.
[Hebeler, Duguet, Lesinski and Schwenk, PRC **80** (2009) 44321]

RESULTS (ISOTOPES)

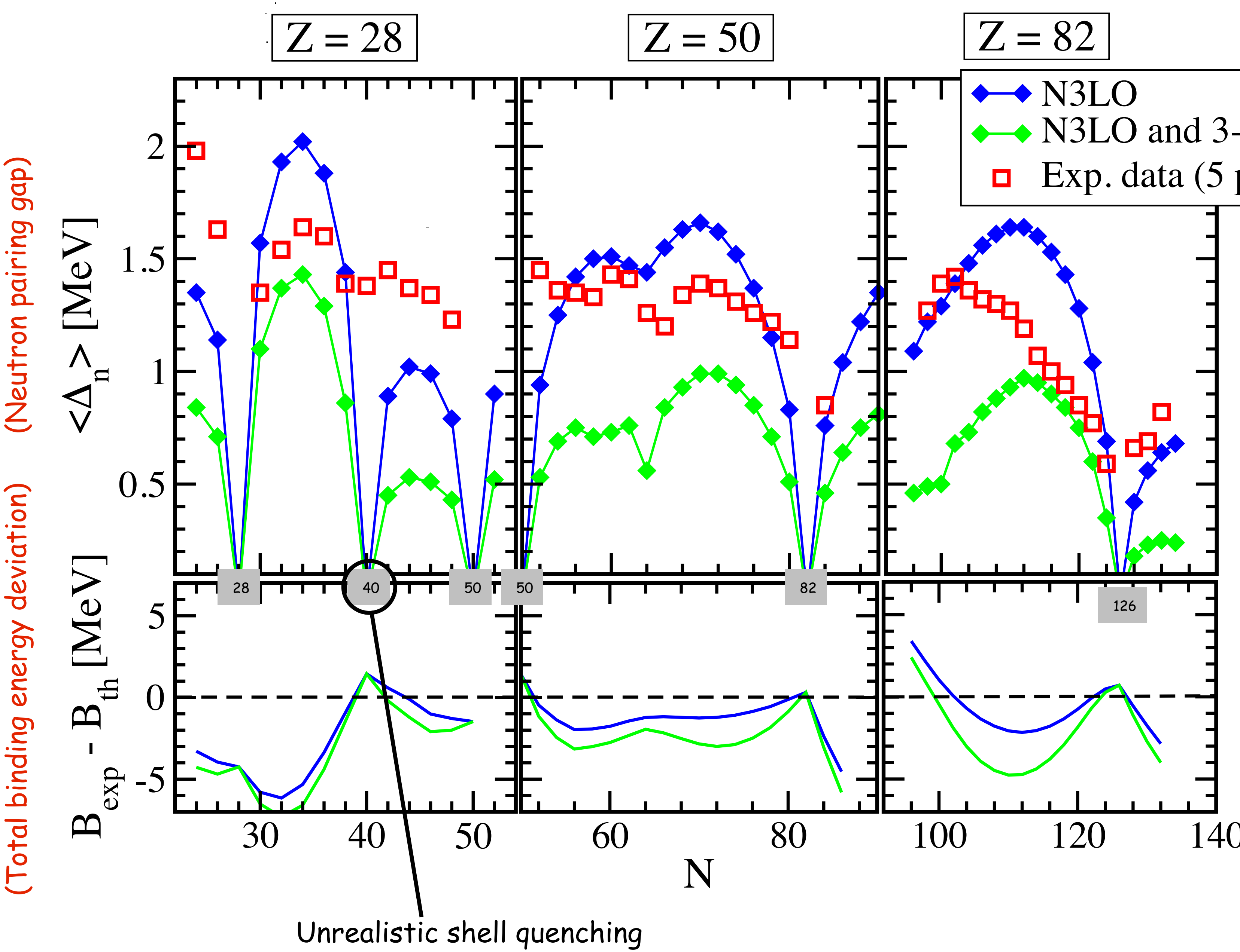

With N3LO pairing gaps in reasonable agreement with exp. data.

With the inclusion of three-body forces pairing gaps are reduced by 30/40% [See also PRC **80** (2009) 044321].

In some cases the pairing gaps collapse because of the "wrong" mean field single particle states.

Binding energies in very good agreement.

FKVW interaction [NPA **770** (2006) 1]

RESULTS (ISOTONES)

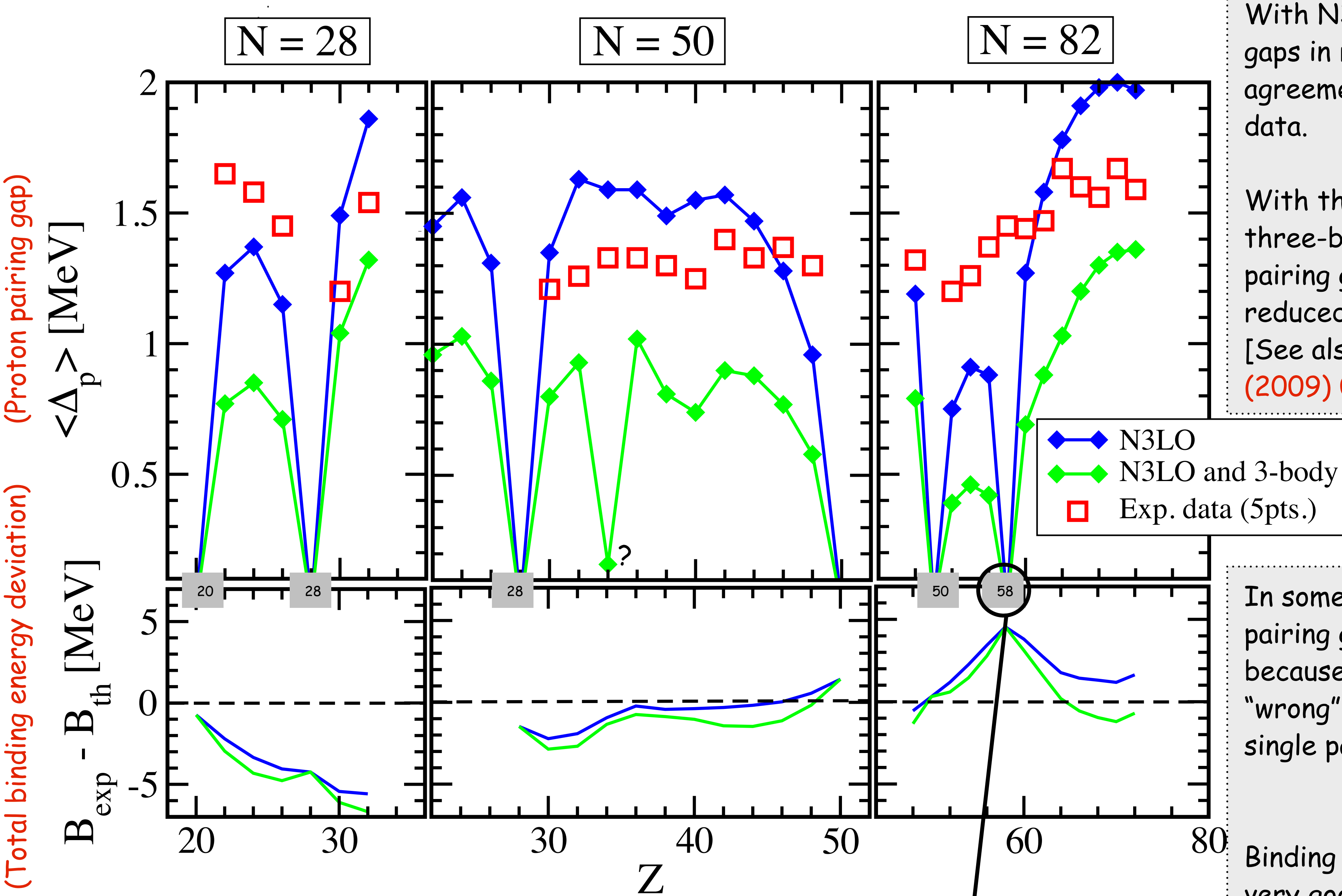

With N3LO pairing gaps in reasonable agreement with exp. data.

With the inclusion of three-body forces pairing gaps are reduced by 30/40 % [See also PRC **80** (2009) 044321].

In some cases the pairing gaps collapse because of the "wrong" mean field single particle states.

Binding energies in very good agreement.

Spurious shell closure
[see Geng et al., CPL **23** (2006) 1139]

FKVW interaction [NPA **770** (2006) 1]

Results (different p-h interactions)

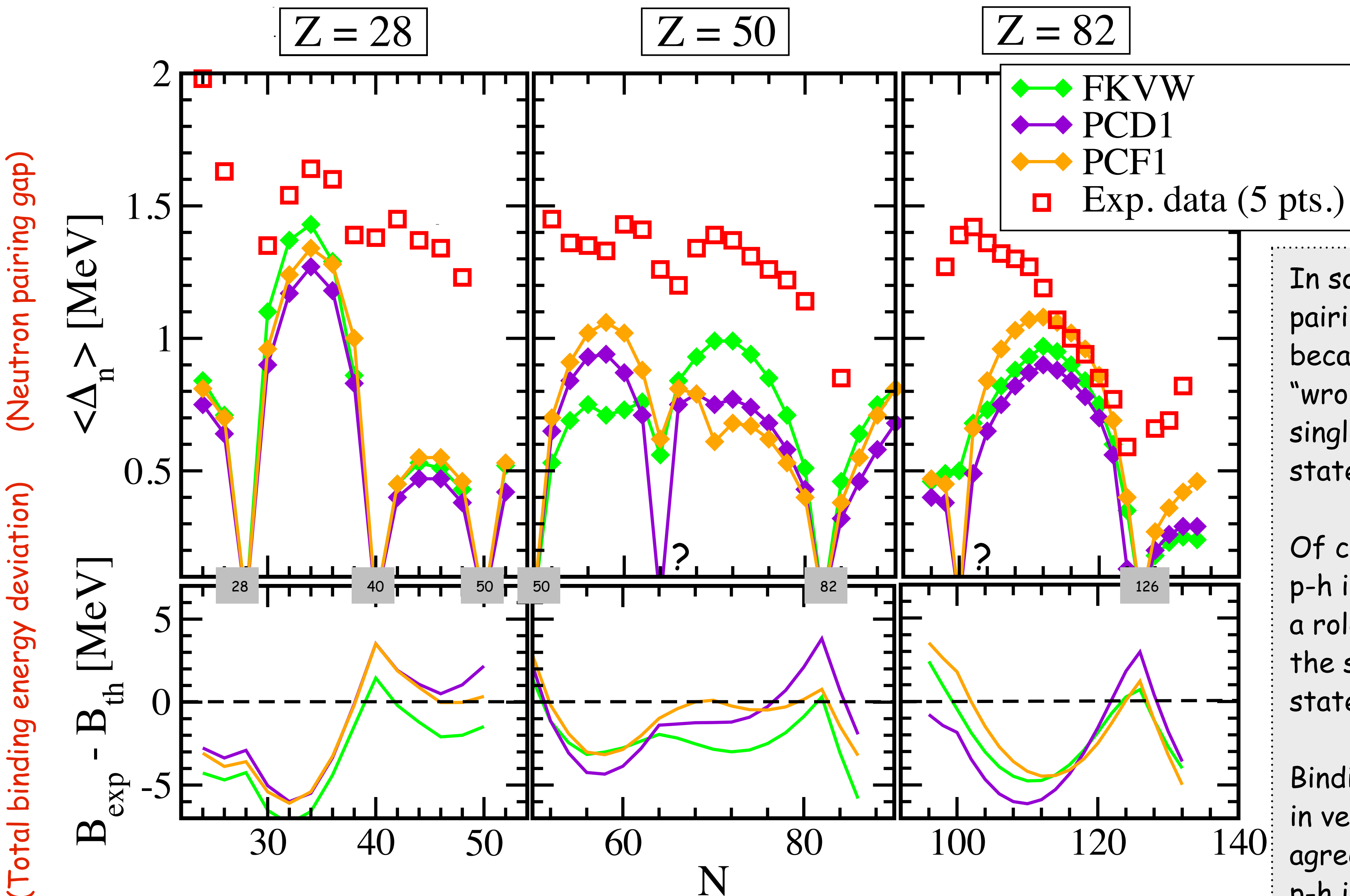

In some cases the pairing gaps collapse because of the "wrong" mean field single particle states.

Of course, different p-h interactions play a role, because of the single-particle states.

Binding energies still in very good agreement for every p-h interaction.

CONCLUSIONS

☑ **Infinite systems**: with the introduction of 3-body forces the pairing gap is reduced in magnitude and shifted towards smaller momenta.

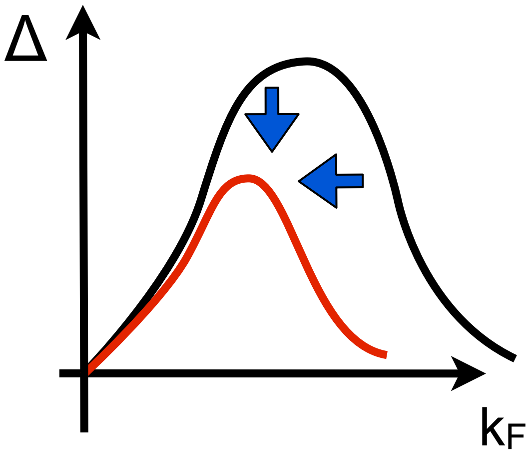

☑ **Finite nuclei**: with the introduction of 3-body forces pairing gaps in finite nuclei are strongly reduced respect to the 2-body case. [See K. Hebeler et al., PRC **80** (2009) 044321 and 1104.2955, T. Duguet et al., nucl-th/1004.2358v1 and references therein]. Additional effects have to be included in order to reproduce empirical data. [Particle vibration Coupling?, Vigezzi et al., nucl-th/1001.1057].

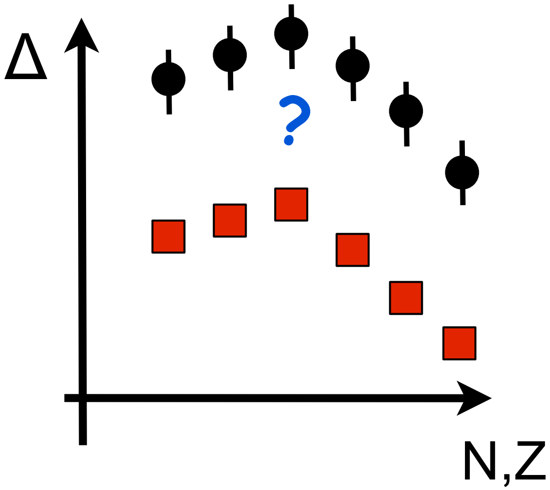

LATEST WORKS

RELATIVISTIC AND NON-RELATIVISTIC MODELS

GROUND-STATE PROPERTIES

IN COLLABORATION

WITH PAVIA, MEUCCI, PACATI E GIUSTI

LECCE, CO' E DE DONNO

GRANADA LALLENA E ANGUIANO

AND ORSAY, GRASSO

SUBMITTED TO PHYS. REV. C

MOTIVATION

We study the predictions of three mean-field theoretical approaches in the description of the ground state properties of some spherical nuclei far from the stability line.

We compare binding energies, single particle spectra, density distributions, charge and neutron radii obtained with different approaches.

The agreement between the results obtained with the three different approaches indicates that these results are more related to the basic hypotheses of the mean-field approach rather than to its implementation in actual calculations.

MODELS

☑ Skyrme

$$\mathcal{E}_{\mathrm{Sk}}^{\mathrm{HF}}=\langle \mathrm{HF}|\hat{v}_{\mathrm{Sk}}|\mathrm{HF}\rangle$$

$$\begin{aligned}\hat{v}_{\mathrm{Sk}}(\mathbf{r}_{12})=&\,t_0(1+x_0\hat{P}_\sigma)\,\delta(\mathbf{r}_{12})+\tfrac{1}{2}t_1(1+x_1\hat{P}_\sigma)[\hat{\mathbf{k}}^{\dagger 2}\delta(\mathbf{r}_{12})\\ &+\delta(\mathbf{r}_{12})\hat{\mathbf{k}}^2]+t_2(1+x_2\hat{P}_\sigma)\,\hat{\mathbf{k}}^\dagger\cdot\delta(\mathbf{r}_{12})\hat{\mathbf{k}}\\ &+\tfrac{1}{6}t_3(1+x_3\hat{P}_\sigma)\,\delta(\mathbf{r}_{12})\rho^\alpha\left(\frac{\mathbf{r}_1+\mathbf{r}_2}{2}\right)\\ &+iW_0(\hat{\boldsymbol{\sigma}}_1+\hat{\boldsymbol{\sigma}}_2)\cdot\hat{\mathbf{k}}^\dagger\delta(\mathbf{r}_{12})\hat{\mathbf{k}},\end{aligned} \quad (5$$

☑ Gogny

$$\begin{aligned}\hat{v}_{\mathrm{Gogny}}(\mathbf{r}_{12})=&\sum_{j=1}^{2}e^{-(\mathbf{r}_{12}/\mu_j)^2}(W_j+B_j\hat{P}_\sigma-H_j\hat{P}_\tau\\ &-M_j\hat{P}_\sigma\hat{P}_\tau)+t_3(1+x_0\hat{P}_\sigma)\,\delta(\mathbf{r}_{12})\\ &\times\rho^\alpha\left(\frac{\mathbf{r}_1+\mathbf{r}_2}{2}\right)+iW_{ls}(\hat{\boldsymbol{\sigma}}_1+\hat{\boldsymbol{\sigma}}_2)\cdot\hat{\mathbf{k}}^\dagger\times\delta(\mathbf{r}_{12})\hat{\mathbf{k}},\end{aligned}$$

☑ RMF (meson-exchange)

$$E=\int d^3r\,\mathcal{E}_{\mathrm{RMF}}+E_{\mathrm{Coul}}+E_{\mathrm{pair}}-E_{\mathrm{cm}},$$

$$\mathcal{E}_{\mathrm{RMF}}=\mathcal{E}_{\mathrm{nucl}}+\mathcal{E}_{\mathrm{meson}}+\mathcal{E}_{\mathrm{coupl}}+\mathcal{E}_{\mathrm{nonl}},$$

$$\mathcal{E}_{\mathrm{nucl}}=\sum_{\alpha=1}^{\Omega}v_\alpha^2\bar{\psi}_\alpha(-i\gamma\cdot\nabla+m_{\mathrm{B}})\,\psi_\alpha,$$

$$\mathcal{E}_{\mathrm{meson}}=\sum_{\mathcal{M}=\sigma,\omega,\rho}\frac{1}{2}\Phi_{\mathcal{M}}(-\Delta+m_{\mathcal{M}})\Phi_{\mathcal{M}}$$

$$\mathcal{E}_{\mathrm{coupl}}=g_\sigma\Phi_\sigma\rho_{s0}+g_\omega\Phi_\omega^\mu\rho_{\mu0}+g_\rho\Phi_\rho^\mu\rho_{\mu,1}$$

Density-dependent coupling

INFINITE SYSTEMS

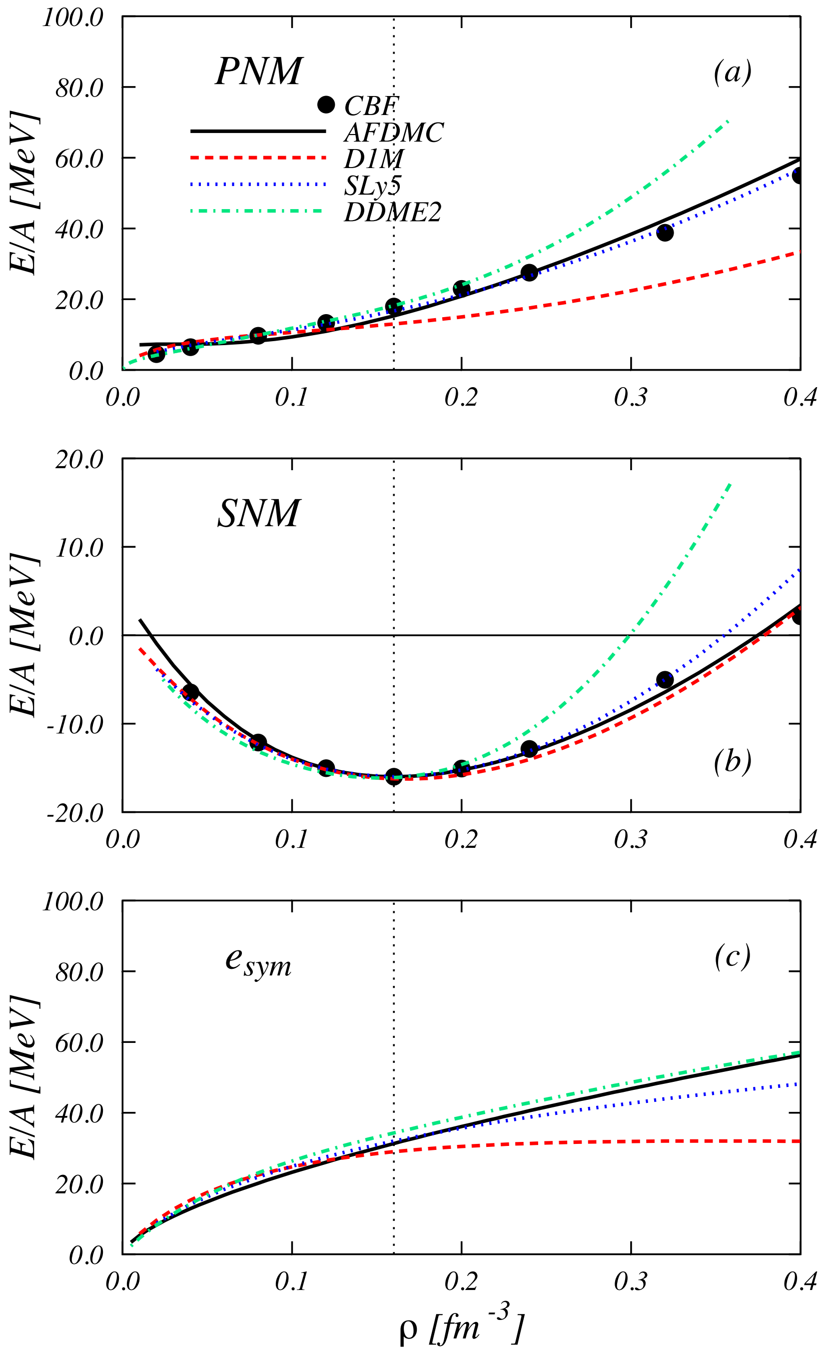

$$e(\rho,\delta) \;=\; e(\rho,0) \;+\; e_{\rm sym}(\rho)\,\delta^2 \;+\; \mathcal{O}(\delta^4)$$

$$e(\rho,0) \;=\; a_V \;+\; \frac{1}{2} K_V\,\epsilon^2 \;+\; \ldots$$

$$K_V \;=\; 9\rho_0^2\,\left.\frac{\partial^2 e(\rho,0)}{\partial\rho^2}\right|_{\rho=\rho_0}$$

$$e_{\rm sym}(\rho) \;=\; a_{\rm sym} \;+\; \mathcal{L}\,\epsilon \;+\; \ldots$$

$$\mathcal{L} \;=\; 3\rho_0\,\left.\frac{\partial e_{sym}(\rho)}{\partial\rho}\right|_{\rho=\rho_0}$$

	exp	AFDMC	CBF	D1M	SLy5	DDME2
ρ_0	0.16 ± 0.01	0.16	0.16	0.16	0.16	0.15
$e(\rho_0,0)$	-16.0 ± 0.1	-16.00	-16.00	-16.01	-15.98	-16.13
K_V	220 ± 30	276	269	217	228	278
$a_{\rm sym}$	30-35	31.3	33.94	29.45	32.66	33.20
$\mathcal{L}$	88 ± 25	60.10	58.08	25.41	48.38	54.74

BINDING ENERGIES

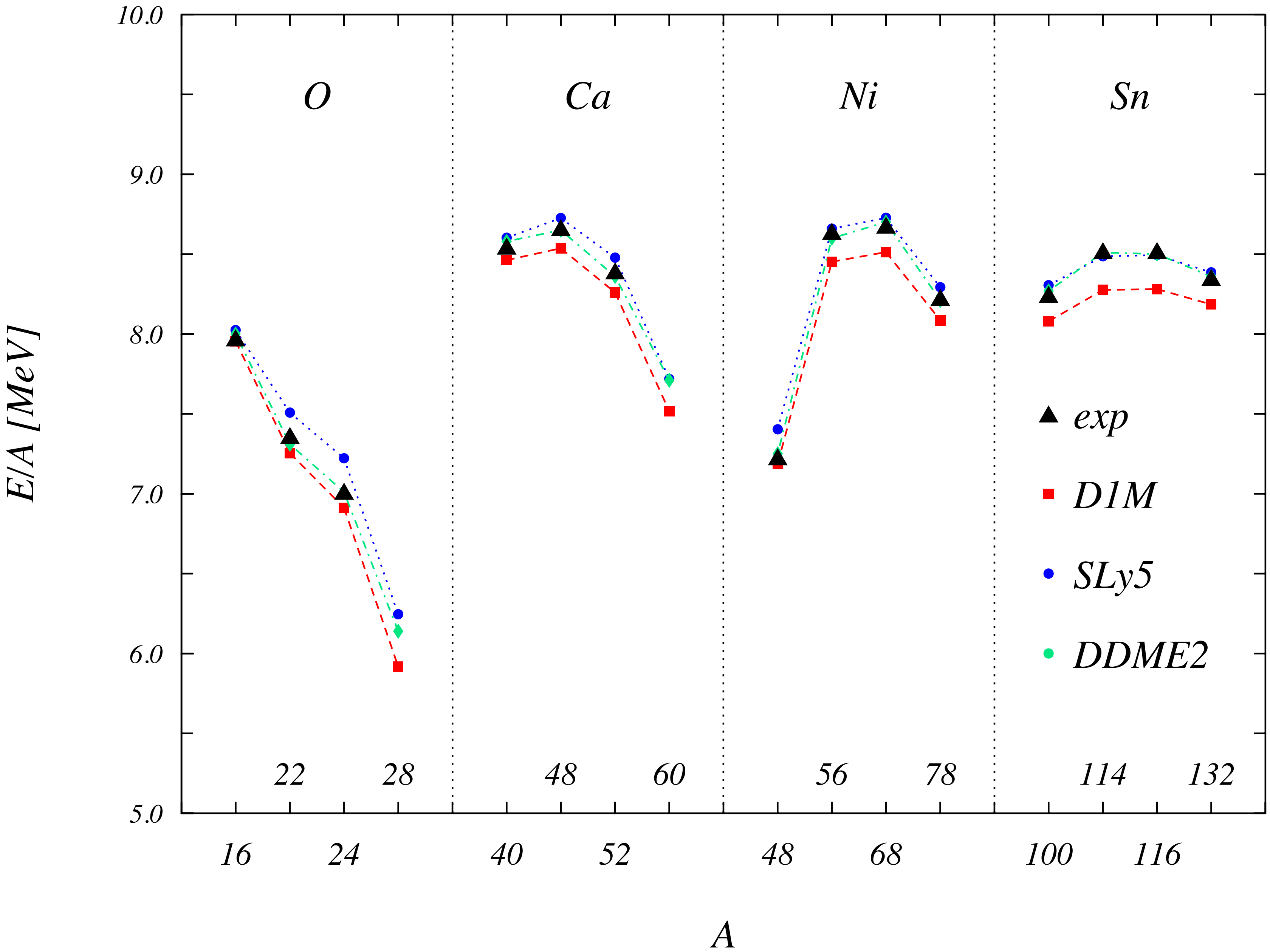

ENERGIES (I)

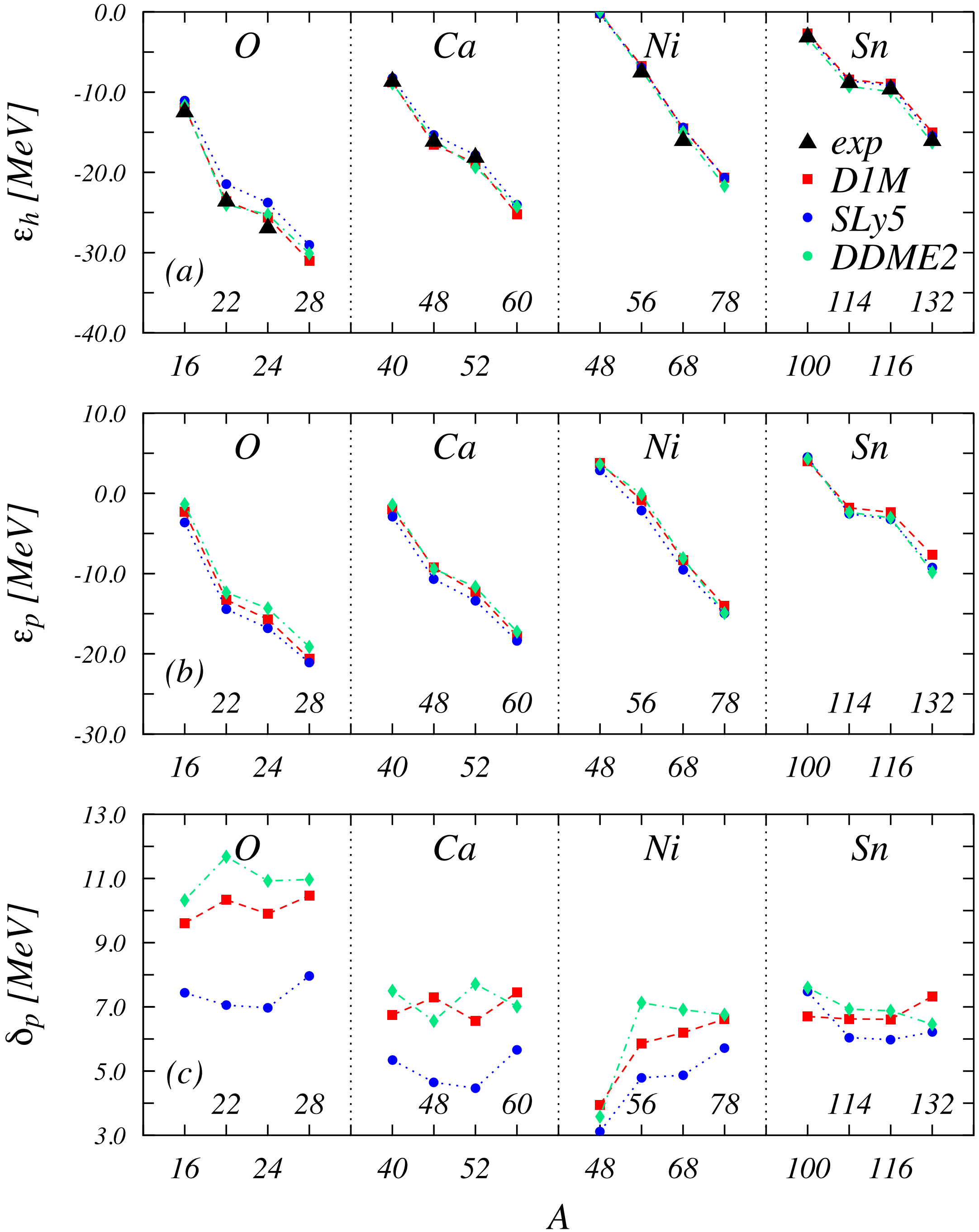

Single particle proton levels below the Fermi surface

Single particle proton levels above the Fermi surface

Proton energy gap $\varepsilon_p - \varepsilon_h$

ENERGIES (II)

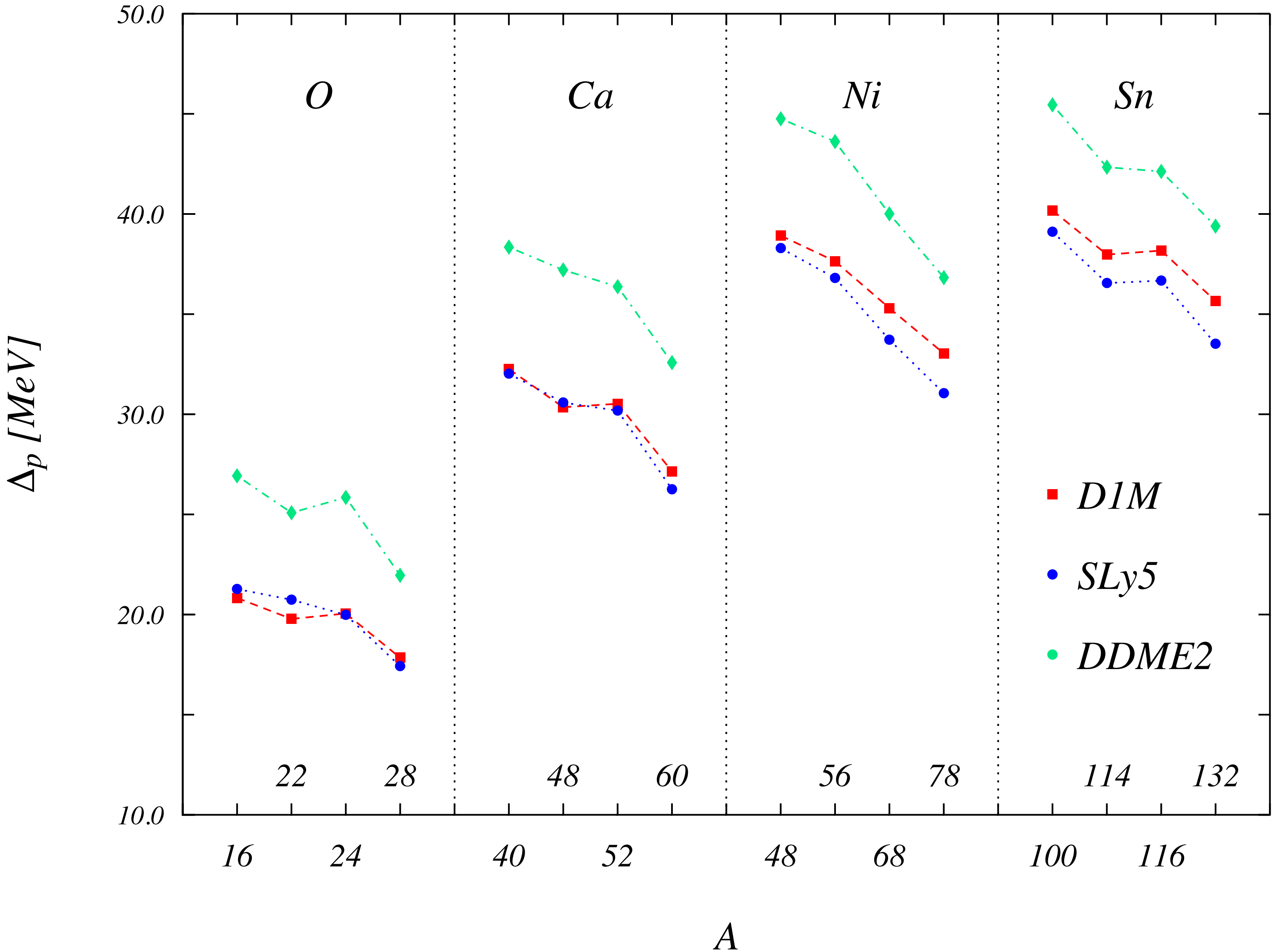

Differences between the s.p. energy of the least bound proton level and that of the $1s_{1/2}$ level, calculated with the three different MF models.

PROTON DISTRIBUTIONS

Proton distributions for the various calcium isotopes

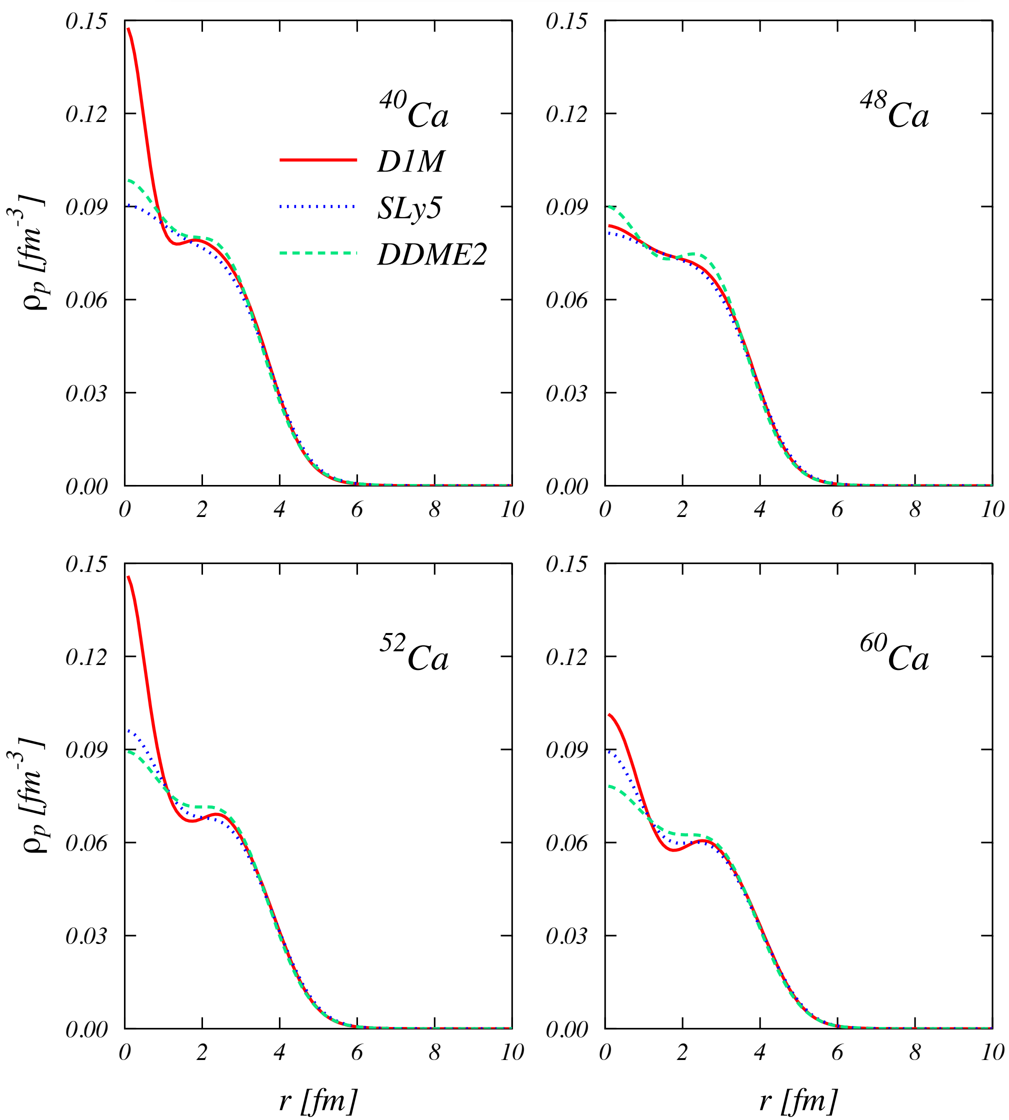

Wave functions of the proton $2s_{1/2}$ levels for the calcium isotopes.

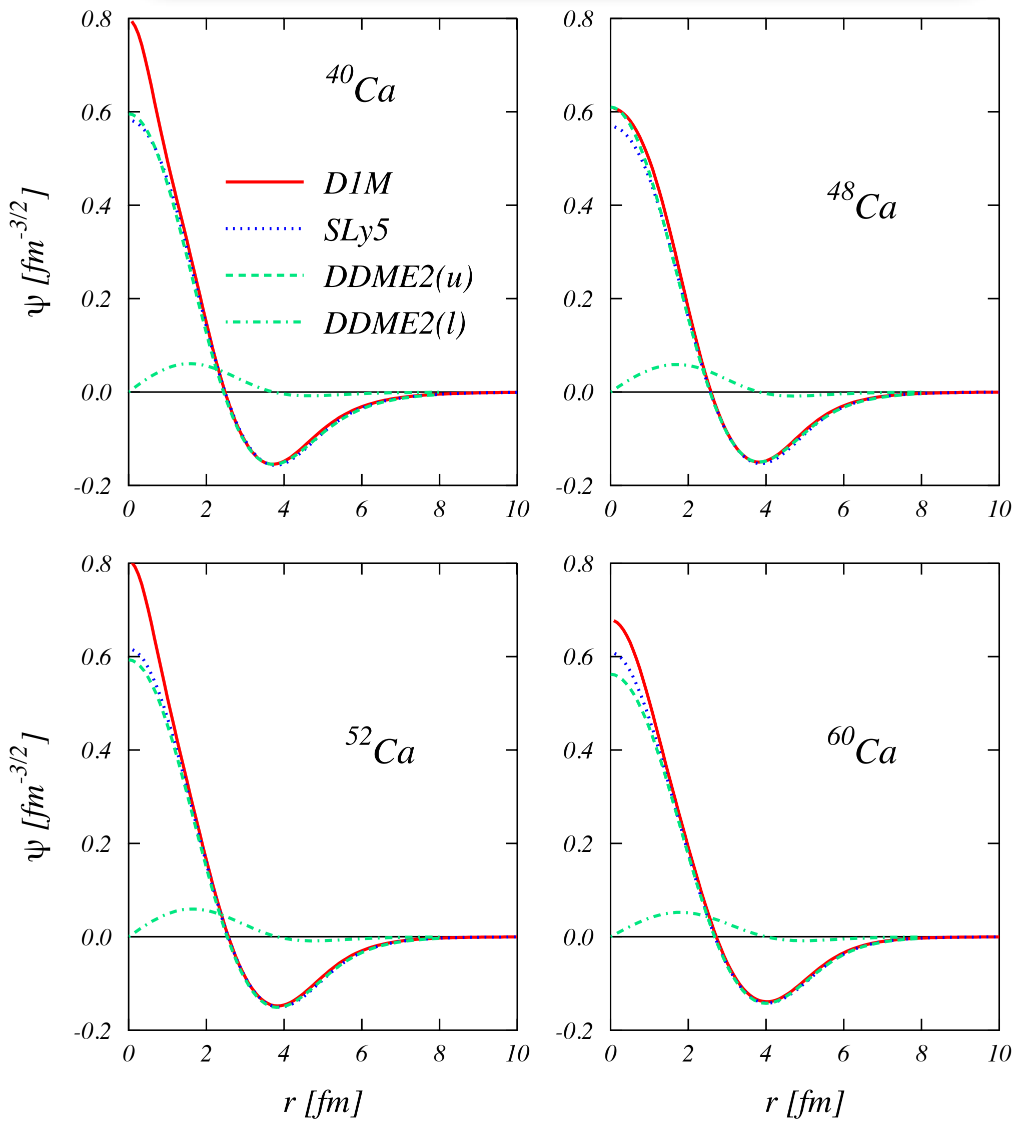

NEUTRON AND MATTER DISTRIBUTIONS

Neutron distributions for the various calcium isotopes

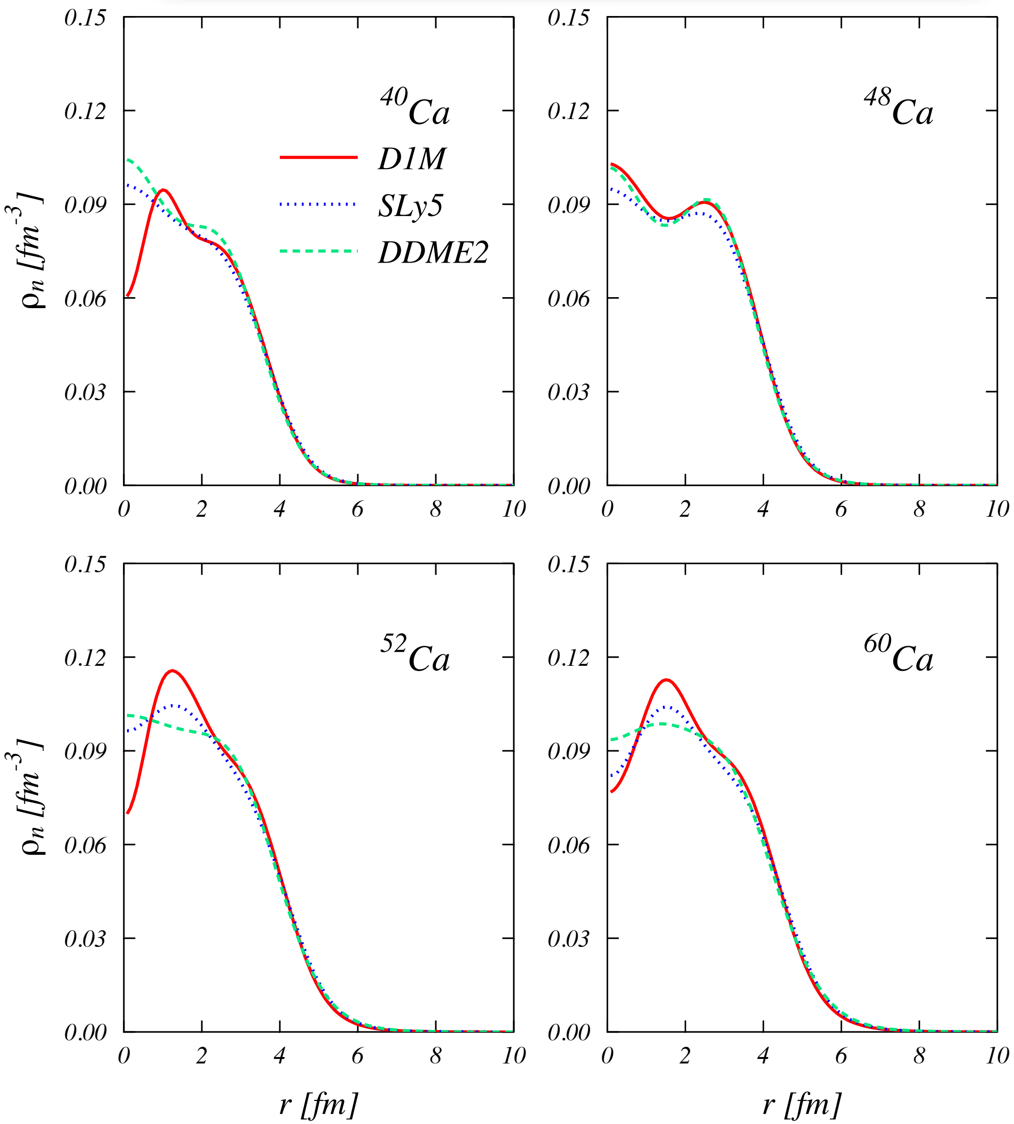

Matter distributions for the various calcium isotopes

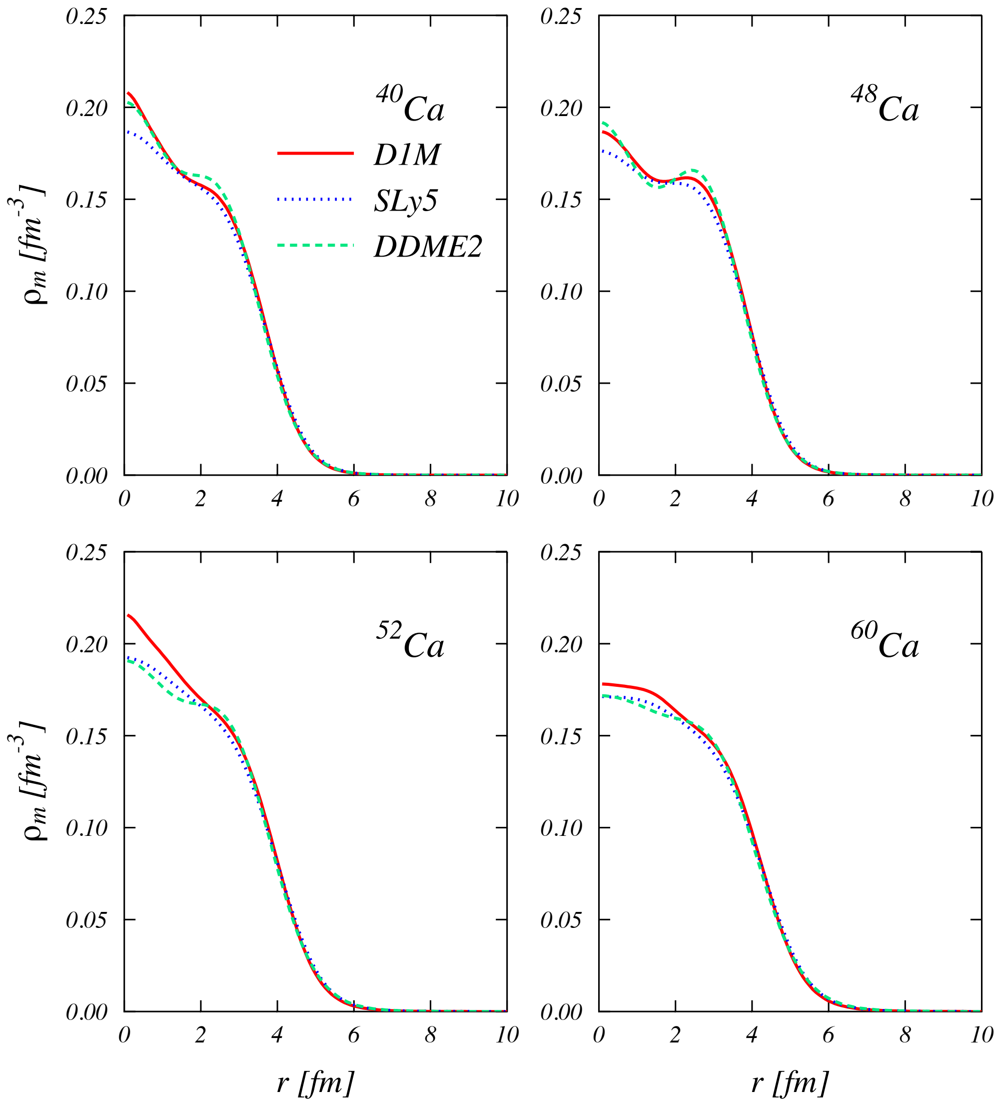

RADII

rms charge radii

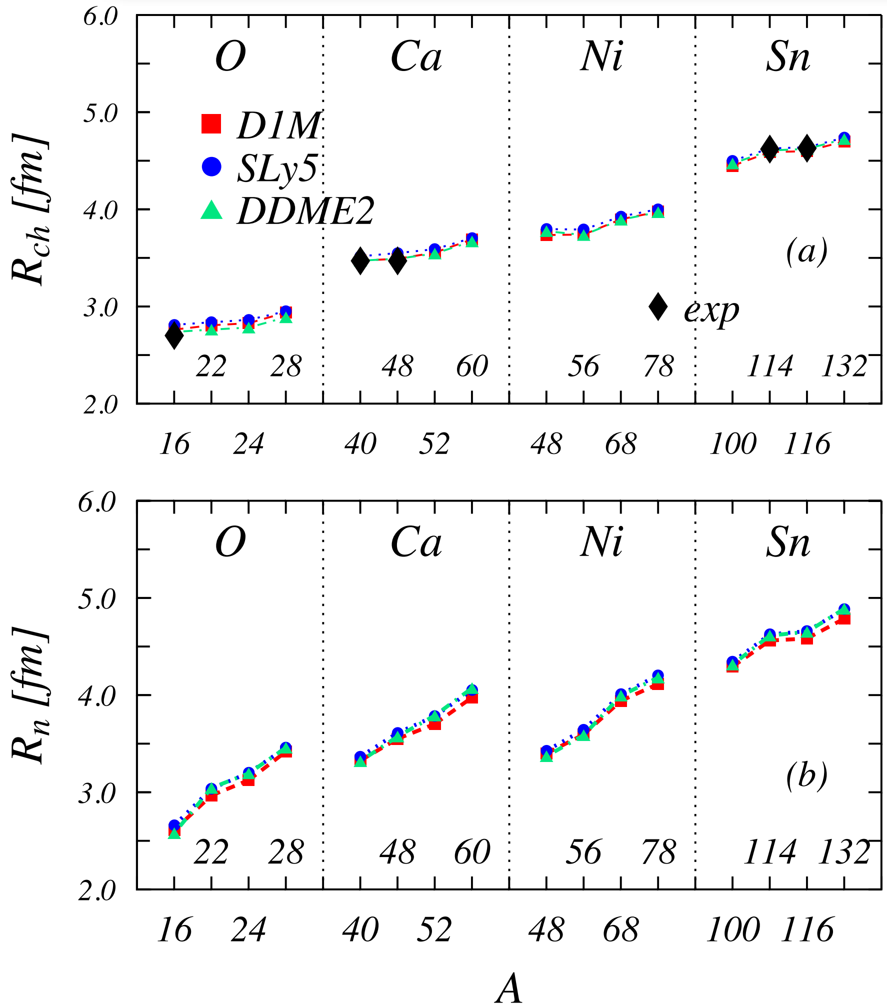

neutron radii

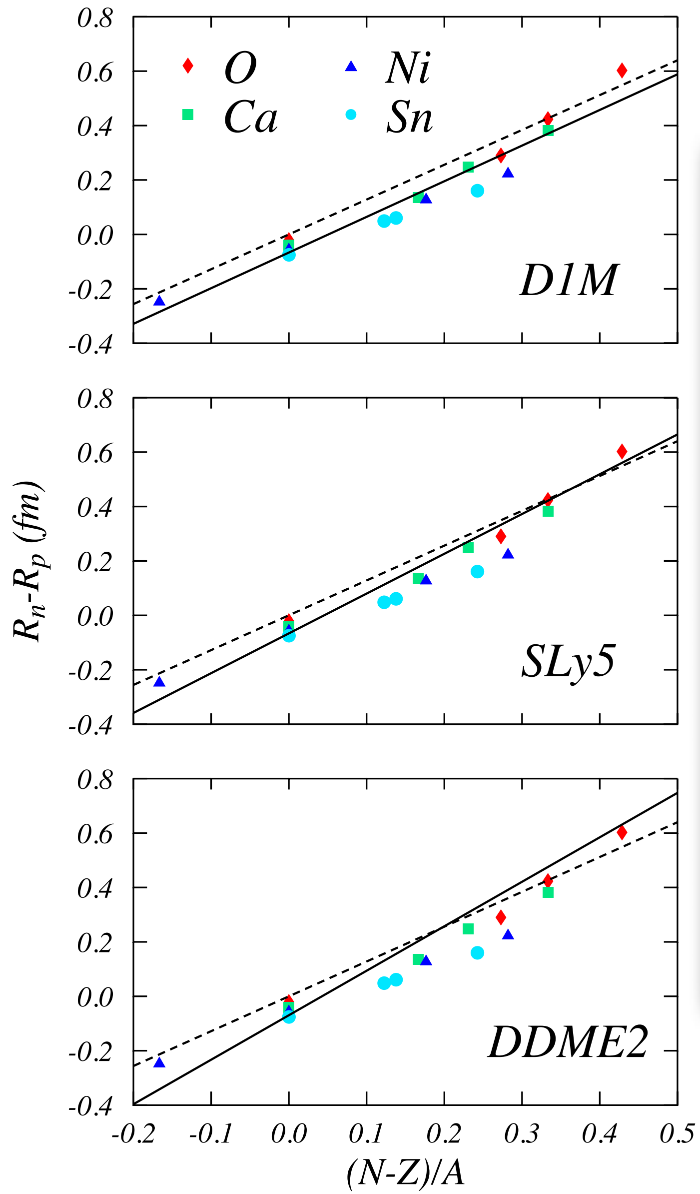

Neutron skins calculated with the three different approaches as a function of the relative neutron excess.

The full lines show a linear fit do the data, the dashed lines present the predictions by Angeli et al.

CONCLUSIONS (I)

1. The properties of infinite nuclear matter at saturation densities are very similar for the three approaches. The only exception is L. Above the saturation point, the behaviors of the EOS are remarkably different, especially in the case of PNM.

2. In our calculations all the 16 nuclei investigated are bound. This MF prediction could be in contrast with the experimental evidence (the neutron drip line for the oxygen isotopes starts with the ^{26}O nucleus, therefore ^{28}O is experimentally an unstable system)

3. The proton s.p. energies around the Fermi surface have similar values for all the three calculations.

4. In each isotopes chain, the energy available to arrange the proton s.p. levels decreases with increasing neutron number. As a consequence the density of states increases.

5. The study of the density distributions indicates a good agreement at the nuclear surface for all the three types of calculations. In the nuclear interior we have observed very different behaviors when the proton and neutron densities are separately considered. These differences in the nuclear center are much smaller when the total matter is considered.

CONCLUSIONS (II)

6. The large differences of the proton distributions in the nuclear interior are due to the **s** proton waves.

7. The values of the charge rms radii are very similar in all the three calculations and agree very well with the available experimental data and with their empirical extrapolations. Our results show a small increase of these radii with the neutron numbers.

8. Neutron skins are larger in light than in heavy nuclei. This is not a trivial geometrical effect.

The most important message emerging from our investigation is the convergence of the results of the 3 MF models for all the nuclei investigated. **This indicates the importance of producing and investigating exotic nuclei**. The comparison between the observed properties and the MF predictions is going to confirm, or not, the MF model itself, and not a specific implementation of it.

MORE SLIDES....

SEPARABLE PAIRING BY Y. TIAN (MORE)

space to the coordinate space and obtain

$$V(\mathbf{r}_1,\mathbf{r}_2,\mathbf{r}'_1,\mathbf{r}'_2) = -\,G\,\delta(\mathbf{R}-\mathbf{R}')\,P(r)P(r')\,\tfrac{1}{2}(1-P^\sigma) \tag{14}$$

where $\mathbf{R} = \frac{1}{2}(\mathbf{r}_1 + \mathbf{r}_2)$ and $\mathbf{r} = \mathbf{r}_1 - \mathbf{r}_2$ are center of mass and relative coordinates respectively, and $P(r)$ is obtained from the Fourier transform of $p(k)$. Using the Gaussian ansatz (12) we find

$$P(r) = \frac{1}{(4\pi a^2)^{3/2}} e^{-\frac{r^2}{4a^2}}. \tag{15}$$

Because of the δ-term in Eq. (14) that insures translational invariance this force is not completely separable in coordinate space. However, the matrix elements of this force can be represented by a sum of a few separable terms in a basis of spherical harmonic oscillator functions.

In order to show this we start from the basis

$$|nljm_j\rangle = \varphi_{nljm_j}(\mathbf{r}) = R_{nl}(r,b)[Y_l(\hat{r}) \otimes \chi_{\frac{1}{2}}]_{jm_j} \tag{16}$$

where $R_{nl}(r,b) = b^{-\frac{3}{2}} R_{nl}(r/b)$ and $[Y_l(\hat{r}) \otimes \chi_{\frac{1}{2}}]_{jm_j}$ represents the wave function in spin and angels coupled to total angular momentum jm_j. The radial wave function has the form

$$R_{nl}(x) = \sqrt{\frac{2n!}{(n+l+\frac{1}{2})!}}\, x^l L_n^{l+\frac{1}{2}}(x^2) e^{-\frac{x^2}{2}} \tag{17}$$

with the radial quantum number $n = 0, 1, \ldots$ and the orbital angular momentum l. The quantity $b = \sqrt{\hbar/(m\omega_0)}$ is the harmonic oscillator length. In the pairing channel we need only the two-particle wave functions coupled to angular momentum $J = 0$ and the projector $\frac{1}{2}(1-P^\sigma)$ restricts us to the quantum numbers $S = L = 0$. Recoupling from the LS- to the jj-scheme therefore leads to the two-particle wave function

$$\begin{aligned} |12\rangle_0 &\equiv |\varphi_{n_1l_1j_1}(\mathbf{r}_1), \varphi_{n_2l_2j_2}(\mathbf{r}_2)\rangle_{J=0} \\ &= \frac{\hat{j}}{\hat{s}\hat{l}} R_{n_1l_1}(r_1,b) R_{n_2l_2}(r_2,b) |\lambda = 0\rangle |S = 0\rangle \end{aligned} \tag{18}$$

with $\hat{j} = \sqrt{2j+1}$ and $s = \frac{1}{2}$. The functions $|\lambda = 0\rangle = [Y_{l_1}(\hat{r}_1) \otimes Y_{l_2}(\hat{r}_2)]_0$ and $|S = 0\rangle = [\chi_{\frac{1}{2}} \otimes \chi_{\frac{1}{2}}]_0$ are the angular and spin wave functions coupled to angular momentum $\lambda = 0$ and spin $S = 0$. All these wave functions are expressed in laboratory coordinates, while the separable pairing interaction in Eq. (14) is expressed in the center of mass frame by the center of mass coordinate $\mathbf{R}$ and the relative coordinates $\mathbf{r}$ of a pair. Therefore we transform to the center of mass frame using Talmi-Moshinsky brackets [59–61]. We use the definition of Baranger [62]

$$|n_1l_1, n_2l_2; \lambda\mu\rangle = \sum_{NLnl} M^{NLnl}_{n_1l_1n_2l_2} |NL, nl; \lambda\mu\rangle \tag{19}$$

where

$$M^{NLnl}_{n_1l_1n_2l_2} = \langle NL, nl, \lambda | n_1l_1, n_2l_2, \lambda\rangle \tag{20}$$

SEPARABLE PAIRING BY Y. TIAN (MORE)

are the Talmi-Moshinsky brackets with the selection rule

$$2N + L + 2n + l = 2n_1 + l_1 + 2n_2 + l_2. \qquad (21)$$

Here we need these bracket only for the case $\lambda = 0$. We therefore can express the wave function (18) in terms of center of mass and relative coordinates

$$|12\rangle_0 = \frac{\hat{j}}{\hat{s}\hat{l}} \sum_{NL} \sum_{nl} M^{NLnl}_{n_1 l_1 n_2 l_2} \times R_{NL}(R, b_R) R_{nl}(r, b_r) |\lambda = 0\rangle |S = 0\rangle \qquad (22)$$

with $|\lambda = 0\rangle = \left[Y_L(\hat{R}) \otimes Y_l(\hat{r})\right]_{\lambda=0}$. The oscillator parameters for the center of mass and the relative coordinates are $b_R = b/\sqrt{2}$ and $b_r = b\sqrt{2}$. Finally we find the pairing matrix elements of the interaction (14)

$$V^0_{121'2'} = \langle n_1 l_1 j_1, n_2 l_2 j_2 | V | n_{1'} l_{1'} j_{1'}, n_{2'} l_{2'} j_{2'} \rangle_{J=0} \qquad (23)$$

as a sum over the quantum numbers N, L, N', L', n, l, n', and l' in Eq. (19). The integration over the center of mass coordinates $\mathbf{R}$ and $\mathbf{R}'$ leads to $N = N'$, $L = L'$. Further restrictions occur through the fact that the sum contains integrals over the relative coordinates of the form

$$\int R_{nl}(r, b_r) Y_{lm}(\hat{r}) P(r) d^3 r. \qquad (24)$$

They vanish for $l \neq 0$ and this leads to $L = l = 0$. The quantum numbers n and n' are determined by the selection rule (21) and we are left with a single sum of separable terms

$$V^0_{121'2'} = -G \sum_N V^N_{12} V^N_{1'2'} \qquad (25)$$

with the single particle matrix elements V^N_{12}. For $l_1 = l_2 = l$, $j_1 = j_2 = j$ we find

$$V^N_{12} = M^{N0n0}_{n_1 l n_2 l} \frac{\hat{j}}{\hat{s}\hat{l}} \int_0^\infty R_{n0}(r, b_r) P(r) r^2 dr. \qquad (26)$$

For a Gaussian ansatz of $P(r)$ in Eq. (15) this integral can be evaluated analytically

$$V^N_{12} = \frac{1}{b^{3/2}} \frac{2^{1/4}}{\pi^{3/4}} \frac{(1-\alpha^2)^n}{(1+\alpha^2)^{n+3/2}} \frac{\hat{j}}{\hat{s}\hat{l}} M^{N0n0}_{n_1 l n_2 l} \frac{\sqrt{(2n+1)!}}{2^{n+1} n!} \qquad (27)$$

where the parameter $\alpha = a/b$ characterizes the width of the function $p(r)$ in units of the oscillator length b and n is given by the selection rule (21) $n = n_1 + n_2 + l - N$.

Thus we find, that the pairing matrix elements for the separable pairing interactions used in the RHB equation can be evaluated by the sum of separable terms in Eq. (25). In order to study the pairing properties in finite nuclei, we solve the RHB equation

$$\begin{pmatrix} h_D - \mu & \Delta \\ \Delta & -h_D + \mu \end{pmatrix} \begin{pmatrix} U \\ V \end{pmatrix}_k = E_k \begin{pmatrix} U \\ V \end{pmatrix}_k \qquad (28)$$

RESULTS FROM DUGUET ET AL. (2)

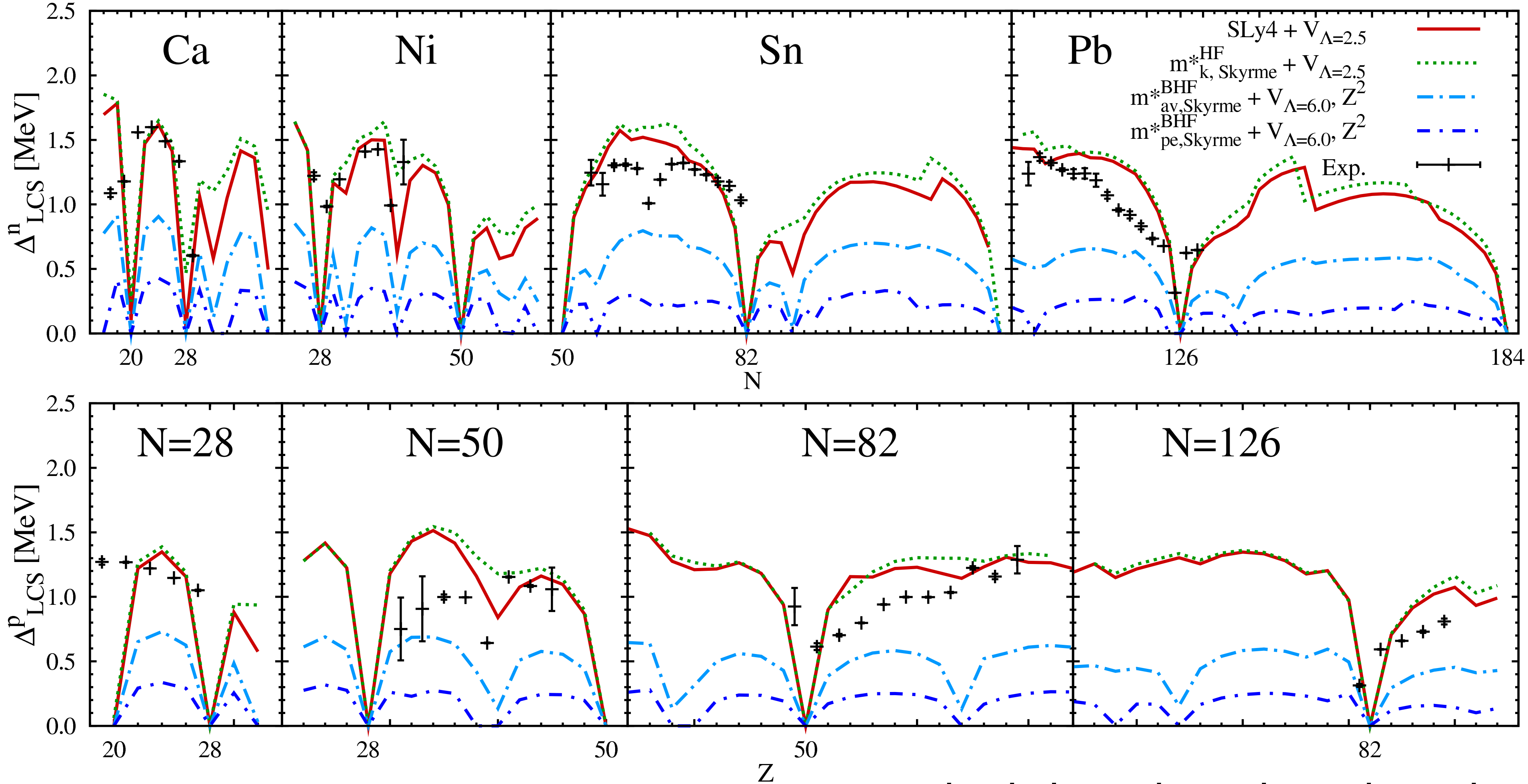

Theoretical gaps are provided by the diagonal pairing matrix element corresponding to the canonical single-particle state whose quasi-particle energy is the lowest.

SLy4 + $V_{\Lambda=2.5}$

$m^{*HF}_{k,\,Skyrme} + V_{\Lambda=2.5}$

$m^{*BHF}_{av,Skyrme} + V_{\Lambda=6.0}, Z^2$

$m^{*BHF}_{pe,Skyrme} + V_{\Lambda=6.0}, Z^2$

Exp.

RESULTS FROM DUGUET ET AL. (3)

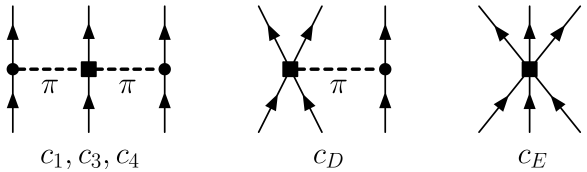

First-order contribution from chiral three-nucleon forces,
2N and 3N accounts only for 70% of the pairing gaps

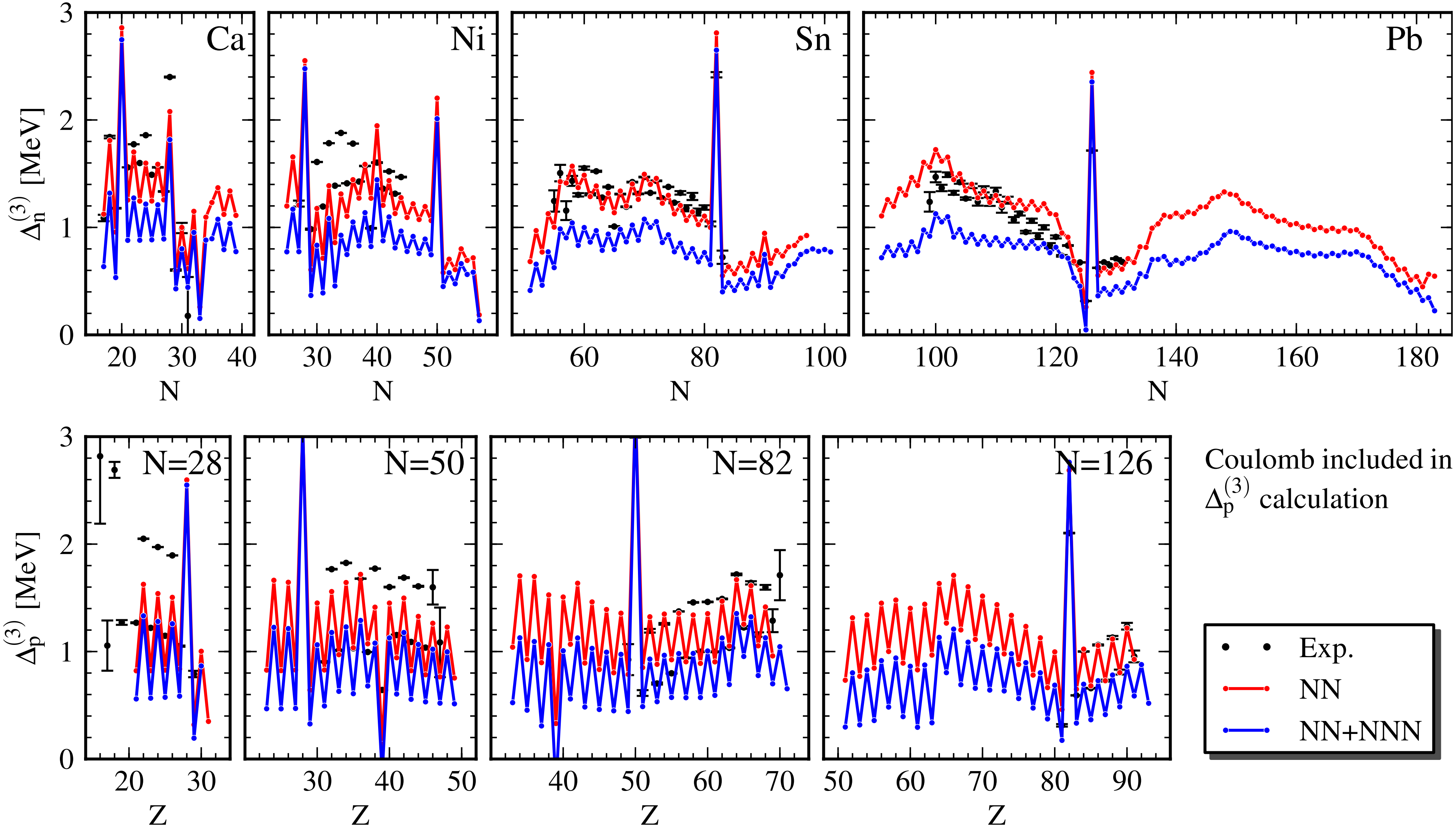

EFFECTIVE MASS M*

Fritsch, Kaiser and Weise,
NPA **750** (2005) 259

Holt, Kaiser and Weise,
nucl-th/**1107.5966**

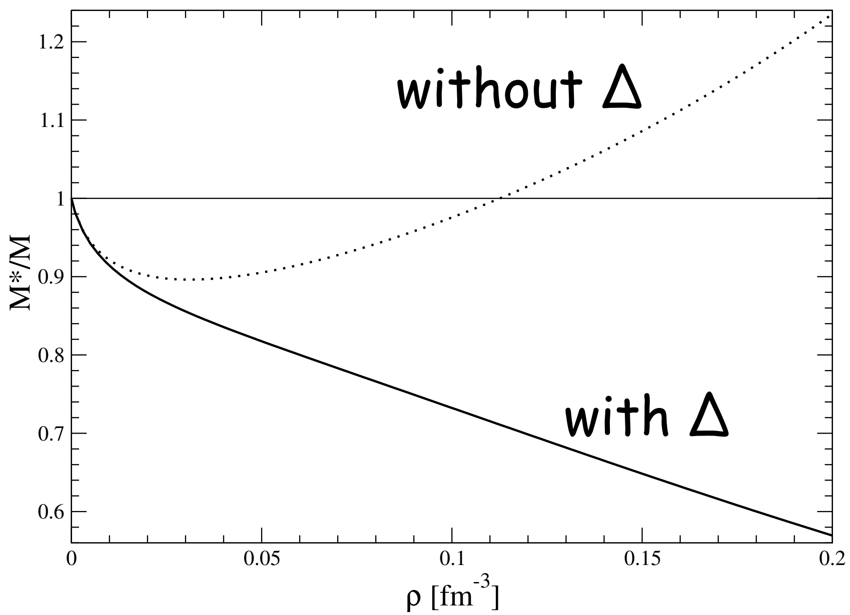

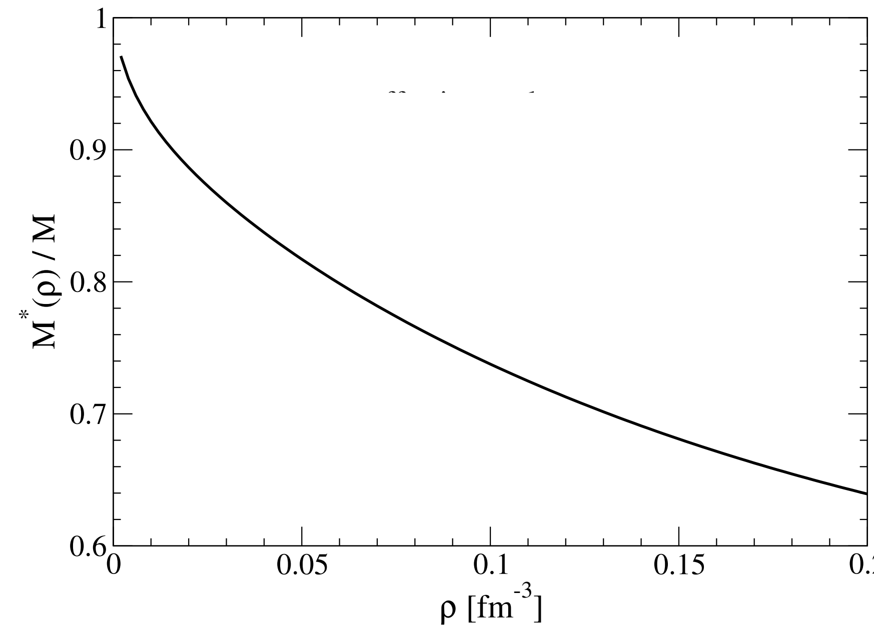

3-loop calculation of nuclear matter in CHPT by including the effects from 2π exchange with single and double virtual Δ excitation.

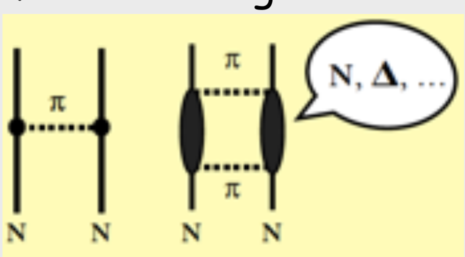

Regularization dependent short-range contributions with NN-contact coupling terms.

The two-body interaction comprises long-range one- and two-pion exchange contributions and a set of contact terms contributing up to fourth power in momenta.

In addition they add the leading order chiral 3N interaction with its parameters c_E, c_D and $c_{1,3,4}$.